The Journal of Experimental Biology 216, 2523-2541

doi:10.1242/jeb.083261

REVIEW

Proximate and ultimate causes of signal diversity in the electric fish *Gymnotus*

W. G. R. Crampton[1,*], A. Rodríguez-Cattáneo[2], N. R. Lovejoy[3] and A. A. Caputi[2,4,*]

[1]Department of Biology, University of Central Florida, 4000 Central Florida Boulevard, Orlando, FL 32816, USA, [2]Departamento de Neurociencias Integrativas y Computacionales, Instituto de Investigaciones Biológicas Clemente Estable, Av. Italia 3318, Montevideo 11600, Uruguay and [3]Department of Biological Sciences, University of Toronto Scarborough, 1265 Military Trail, Toronto, ON, Canada, M1C 1A4

*Authors for correspondence (crampton@ucf.edu; caputiangel@gmail.com)

Summary

A complete understanding of animal signal evolution necessitates analyses of both the proximate (e.g. anatomical and physiological) mechanisms of signal generation and reception, and the ultimate (i.e. evolutionary) mechanisms underlying adaptation and diversification. Here we summarize the results of a synthetic study of electric diversity in the species-rich neotropical electric fish genus *Gymnotus*. Our study integrates two research directions. The first examines the proximate causes of diversity in the electric organ discharge (EOD) – which is the carrier of both the communication and electrolocation signal of electric fishes – *via* descriptions of the intrinsic properties of electrocytes, electrocyte innervation, electric organ anatomy and the neural coordination of the discharge (among other parameters). The second seeks to understand the ultimate causes of signal diversity – *via* a continent-wide survey of species diversity, species-level phylogenetic reconstructions and field-recorded head-to-tail EOD (ht-EOD) waveforms (a common procedure for characterizing the communication component of electric fish EODs). At the proximate level, a comparative morpho-functional survey of electric organ anatomy and the electromotive force pattern of the EOD for 11 species (representing most major clades) revealed four distinct groups of species, each corresponding to a discrete area of the phylogeny of the genus and to a distinct type of ht-EOD waveform. At the ultimate level, our analyses (which emphasize the ht-EOD) allowed us to conclude that selective forces from the abiotic environment have had minimal impact on the communication component of the EOD. In contrast, selective forces of a biotic nature – imposed by electroreceptive predators, reproductive interference from heterospecific congeners, and sexual selection – may be important sources of diversifying selection on *Gymnotus* signals.

Key words: communication, electrolocation, electroreception, gymnotiform, neotropical.

Received 26 November 2012; Accepted 17 January 2013

Introduction

The weakly electric fishes of the neotropics (Gymnotiformes) and tropical Africa (Mormyriformes) produce simple, stereotyped electric signals that are carried by electric fields resulting from an electric organ discharge (EOD). A full understanding of the evolution of these signals necessitates an approach that integrates the 'proximate' (i.e. anatomical, physiological and other functional bases of signal generation and reception) with the 'ultimate' (i.e. evolutionary) mechanisms underlying adaptation and diversification (*sensu* Mayr, 1961). At the proximate level, substantial progress has been made for a small number of model species (e.g. the gymnotiforms *Gymnotus omarorum*, *Brachyhypopomus gauderio* and *Apteronotus albifrons*, and the mormyrid *Gnathonemus petersii*) in understanding the physiological and anatomical bases of electric signal generation and reception, the hormonal basis of signal plasticity, and the nature of signal modulations in sexual and territorial communication (Bullock et al., 2005). Meanwhile, progress has been made for several mormyriform and gymnotiform groups in circumscribing the diversity, distribution and natural history of species, hypothesizing phylogenetic interrelationships among these species, and describing signal diversity.

The integration of data from multiple fields is beginning to provide us with a holistic view of signal diversity and evolution, but efforts to date have largely focused on broad patterns among disparate groups, rather than a comparative species-level approach for taxa within a phylogenetically well-resolved clade. A notable exception is the mormyrid genus *Paramormyrops*, which as a consequence of decades of study by the Hopkins laboratory at Cornell University, is a paradigmatic group for understanding species and signal evolution in the context of a rapidly evolving vertebrate species flock (e.g. Arnegard et al., 2010a).

Here we summarize our attempts to integrate proximate and ultimate studies of signal and species diversity in a gymnotiform clade, the banded knifefish genus *Gymnotus*. This genus includes 37 described species, distributed in lowland freshwater systems from Uruguay to southern Mexico, with maximum species diversity occurring in the Amazon and Orinoco basins (Crampton, 2011). *Gymnotus* species are nocturnal predators of aquatic invertebrates or small fishes and occur in a variety of habitats, including slow-flowing streams, swamps and floodplains, where they usually inhabit tangled substrates such as vegetation, root masses and leaf litter (Crampton, 1998). Adapted to live in such a geometrically complex environment, *Gymnotus* utilize pulsed EODs and an array of cutaneous electroreceptors both to sense the presence of nearby objects (Aguilera and Caputi, 2003; Caputi et al., 2003) and to communicate (Black-Cleworth, 1970; Westby, 1974). *Gymnotus*

exhibit considerable diversity of electric organ (EO) structure across their distributional range, and this diversity is translated into the spatiotemporal pattern of the EOD-associated electric field (Rodríguez-Cattáneo and Caputi, 2009; Rodríguez-Cattáneo et al., 2013; Rodríguez-Cattáneo et al., 2008). There is increasing evidence that the conspecific-detected EOD waveform serves as a communication signal, and contains information that may mediate interspecific, and even individual, recognition in *Gymnotus* (Aguilera et al., 2001; Crampton and Albert, 2006; Crampton et al., 2008; Crampton et al., 2011; McGregor and Westby, 1993). *Gymnotus* are also known to form species-rich local communities in which EOD waveforms are divergent among species and are presumed to play an important role in pre-zygotic reproductive isolation (Crampton et al., 2008; Crampton et al., 2011).

Our understanding of signal diversity in *Gymnotus* is currently advancing on two fronts, corresponding to the efforts of two research teams. The first, coordinated by A. Caputi, seeks to understand the proximate causes of electric signal diversity – including the underlying intrinsic properties of electrocytes, electrocyte innervation and EO anatomy, the neural coordination of the discharge, and the ontogeny of the EO. This work represents the continuation of a series of seminal studies on signal generation, signal reception and central nervous system processing (in the context of both electrolocation and communication) for a single model species, *Gymnotus omarorum*, initiated in Uruguay during the 1980s by O. Trujillo-Cenóz, O. Macadar and colleagues. The second front, led by J. Albert, W. Crampton and N. Lovejoy, is seeking to understand the 'ultimate' causes of signal diversity *via* a long-term survey of the species and electric signal diversity of *Gymnotus* across its entire distribution, and using species-level phylogenetic reconstructions. Here the aim is to evaluate the importance of phenomena that are known to mold signal evolution in other animal groups, including selection from predators, reproductive interference, sexual selection, sensory drive from the physical environment, and non-adaptive drift (Albert et al., 2005; Crampton, 2006; Crampton, 2011; Crampton and Albert, 2006; Crampton et al., 2011; Lovejoy et al., 2010).

In this review we provide an integrated view of these proximate and ultimate approaches. The first section provides the non-specialist reader with a review of the taxonomy and phylogeny of *Gymnotus*, reviews the diversity of field-recorded EOD waveforms among 30 *Gymnotus* taxa, and provides a classification of these waveforms. The second section reviews the proximate bases of diversity of the EOD. Here we summarize phylogenetic patterns in characters gleaned from a detailed morpho-functional survey of electrogenesis in 11 species (including representatives of many of the major clades in the genus, and including the paradigmatic species, *G. omarorum*). In the third section, we review the ultimate bases of signal diversity – describing some of the known or postulated extrinsic selective forces acting on EOD signal diversity. Our long-term intention is to develop *Gymnotus* as a new model for understanding signal evolution.

Our findings are likely to show many interesting convergences and parallels with the *Paramormyrops* system of Africa, but we also expect *Gymnotus* to yield valuable new perspectives. In the first place, the EOD-associated fields of *Gymnotus* result from the weighted sum of multiple sources – generating heterogeneous temporal waveforms along the EO – while mormyrid EOD-associated fields are generated from a small EO in the caudal peduncle that functions as a highly localized source (likewise, there are many important differences in electroreception between gymnotiforms and mormyriforms, despite a remarkable overall convergence) (Caputi and Nogueira, 2012). Also, unlike *Paramormyrops*, which diversified relatively rapidly within a confined geographical range (i.e. forming a species flock) (Sullivan et al., 2002), *Gymnotus* appears to have evolved over a much slower time frame, and at a much wider geographical scale, encompassing all of lowland continental South and Central America (Albert et al., 2005; Crampton, 2011).

Taxonomy, phylogeny and head-to-tail recorded EOD diversity in *Gymnotus*

Taxonomy

Our understanding of the diversity and distributions of species in the genus *Gymnotus* has improved dramatically over the last two decades, mirroring the situation for many other neotropical fish groups (Crampton, 2011). The first reported species of *Gymnotus* was *G. carapo*, described by Linnaeus in 1758 from material collected in Suriname (Albert and Crampton, 2003). By 1990, only six more species had been described, and many species were incorrectly ascribed to *G. carapo* in the electric fish and ecological literature (Albert and Crampton, 2003). A notable example is the model species for functional investigations of electrogenesis and electroreception studied in Uruguay, which was only recently described as *G. omarorum* (Richer-de-Forges et al., 2009). The discovery of three new sympatric species from Venezuela (Mago-Leccia, 1994), and of multiple new sympatric species from the Tefé region of the lowland Amazon basin (Albert and Crampton, 2001; Crampton et al., 2005), hinted at a hitherto unseen diversity in the genus. This stimulated a continent-wide search by Albert, Crampton and colleagues, and led to the discovery of many additional new species, bringing diversity in the genus to 37 species by 2012. These species are listed in Table 1, with their geographical and ecological distributions. *Gymnotus* is now the most diverse of all gymnotiform (and mormyriform) genera, and many additional species of *Gymnotus* await formal description (a doctoral thesis underway in the Albert laboratory will report an additional 14 species). Total diversity in the genus will likely reach or even exceed 70 species.

Phylogeny

Albert et al. (Albert et al., 2005) presented a morphological phylogeny for *Gymnotus* which included 31 species, and Lovejoy et al. (Lovejoy et al., 2010) presented a phylogeny for 18 species based on morphology and both nuclear (*rag2*) and mitochondrial genes (*Cytochrome b* and *16S rRNA*). More recently, Brochu (Brochu, 2011) presented the most complete molecular phylogeny to date, which included 28 *Gymnotus* species, and is based on nearly 4 kb of nucleotide data from two nuclear (*rag2* and *zic1*) and two mitochondrial genes (*Cytochrome b* and *16S rRNA*). The tree topology used in Fig. 1 is based on the data presented in Brochu (Brochu, 2011).

Comparison of these three studies (Albert et al., 2005; Brochu, 2011; Lovejoy et al., 2010) shows that several aspects of the phylogeny of the Gymnotidae are relatively stable, and not expected to change with the addition of new species and new molecular and morphological data. These include the position of the monotypic strongly electric eel genus *Electrophorus* (represented by *E. electricus*) as the sister taxon to *Gymnotus*, and the delineation of several well-supported clades of *Gymnotus* species: the *G. coatesi* and *G. cataniapo* clades [which correspond to the G1 and G2 clades of Lovejoy et al. (Lovejoy et al., 2010)], and also the *G. henni*, *G. cylindricus* and *G. carapo* clades (Fig. 1). To simplify our discussions, we subdivide the four main clades

Table 1. Thirty-seven described and six additional undescribed species of *Gymnotus*, with affiliation to clades and geographical distribution, maximum total length (TL), availability of molecular data for determining phylogenetic position (Mol.), head-to-tail EOD category (ht-EOD), morpho-functional group (Func.) and ecological distribution relative to electrical conductivity (EC) and dissolved oxygen (DO)

Clade/Species	Region	TL (mm)	Mol.	Ht-EOD	Func.	EC	DO
***Gymnotus coatesi* clade**							
G. coatesi LaMonte 1935	LA, UA	210	+	1		Low	Normoxic
G. coropinae Hoedeman 1962	GU, OR, LA, RN, MD, UA	173	+	1	I	Low	Normoxic
G. javari Albert, Crampton & Hagedorn 2003	UA	240	+	1	I	Low	Normoxic
G. jonasi Albert & Crampton 2001	UA	135	+	1		High	Hypoxic
G. melanopleura Albert & Crampton 2001	UA	99				High	Hypoxic
G. onca Albert & Crampton 2001	UA	116				High	Hypoxic
G. stenoleucus Mago-Leccia 1994	OR, RN	171	+	1		Low	Normoxic
***Gymnotus pantherinus* clade**							
G. pantherinus (Steindachner 1908)	SE	200	+	2		Low	Normoxic
***Gymnotus cataniapo* clade**							
G. anguillaris Hoedeman 1962	GU	302	+[a]			Low	Normoxic
G. cataniapo Mago-Leccia 1994	OR, RN	323	+	2		Low	Normoxic
G. n. sp. FRI	UA	148	+	2		Low	Hypoxic
G. pedanopterus Mago-Leccia 1994	OR, RN	281	+	3		Low	Normoxic
***Gymnotus henni* clade**							
G. esmeraldas Albert & Crampton 2003[b]	PS	355				High	Normoxic?
G. henni Albert, Crampton & Maldonado 2003	PS	333	+	4		High	Normoxic?
G. tigre Albert & Crampton 2003	LA, UA	411	+	2	II	High	Hypoxic
***Gymnotus cylindricus* clade**							
G. cylindricus LaMonte 1935	MA	261	+	4		High	Normoxic
G. maculosus Albert & Miller 1995	MA	260	+	4		High	Normoxic
G. panamensis Albert & Crampton 2003	MA	234	+	2		High	Normoxic
***Gymnotus carapo* clade**							
Gymnotus carapo-A clade							
G. curupira Crampton, Thorsen & Albert 2005	UA	239	+	2	II	Low	Hypoxic
G. chaviro Maxime & Albert 2009	UA	275	+			High	Hypoxic
G. obscurus Crampton, Thorsen & Albert 2005	UA	215	+	4	IV	High	Hypoxic
G. n. sp. ALT	MD	302	+	2		Low	Normoxic
G. pantanal Fernandes et al. 2005	PA	251	+	2		?	?
G. varzea Crampton, Thorsen & Albert 2003	UA	285	+	2	II	High	Hypoxic
Gymnotus carapo-B clade							
G. mamiraua Albert & Crampton 2001	LA, UA	244	+	2		High	Hypoxic
G. n. sp. ITU	PA	301	+	2	II	High	Normoxic
G. omarorum Richer-de-Forges et al. 2009	PA, SE	254	+	2	II	High	Normoxic
Gymnotus carapo-C clade							
G. ardilai Maldonado-Ocampo & Albert 2004	MG	430	+	2		High	Normoxic
G. carapo OR	OR	317	+	2		High	Eurytopic
G. choco Albert et al. 2003	PS	350	+			High?	Normoxic
Gymnotus carapo-D clade							
G. arapaima Albert & Crampton 2001	MD, RN, UA	545	+	3		Eurytopic	Eurytopic
G. bahianus Campos da Paz & Costa 1996	NE	241	+			?	?
G. carapo (SU) Linnaeus 1758	OR, GU, LA, MD, PI, UA	364	+	3	III	Eurytopic	Eurytopic
G. carapo CA	UA	300	+	3		Eurytopic	Eurytopic
G. carapo WA[c]	UA	335	+	3	III	Eurytopic	Eurytopic
G. sylvius Albert et al. 1999	PA, SE	425	+	3	III	Eurytopic	Eurytopic
G. ucamara Crampton, Lovejoy & Albert 2003	UA	300	+	3		Eurytopic	Eurytopic
Phylogenetic position not determined							
G. capanema Milhomem et al. 2012	LA	179		2		Low	Normoxic
G. chimarrao Cognato et al. 2007	PA	237		2		High	Normoxic
G. diamantinensis Campos da Paz 2002	LA	125				Low	Normoxic
G. inaequilabiatus (Valenciennes 1847)	PA	998				High	?
G. paraguensis Albert & Crampton 2003	PA	240				?	?
G. tiquie Maxime, Lima & Albert 2011	RN	240				Low	Normoxic

Geographical regions are: GU, Guianas including Suriname (SU); LA, Lower Amazon (downstream of Manaus); MA, Middle America; MD, Madeira; MG, Magdalena; NE, northeast drainages of Brazil from São Francisco to Jequitinhonha; OR, Orinoco; PA, Paraná-Paraguay; PI, Piauí, including Itapicuru and Parnaíba; PS, Pacific slope; SE, southeast coastal drainages of Brazil and Uruguay, south of Jequitinhonha; RN, Rio Negro + Branco; UA, Central Amazon (CA, from Leticia to Manaus) + Western Amazon (WA, upstream of Leticia).

Availability of molecular data is based on Brochu (Brochu, 2011).

EC: low, <ca. 30 μS cm^{-1}; high, ca. 100–300 μS cm^{-1}.

DO: Normoxic, permanently normoxic; Hypoxic, perennially or seasonally hypoxic/anoxic.

Notes:

[a]The sequenced specimen of *G. anguillaris* is of uncertain identity and as such the position of *G. anguillaris* is at present uncertain.

[b]Phylogenetic position from Albert et al. (Albert et al., 2005).

[c]Corresponds to *G.* sp. 'carapo PE' in Rodríguez-Cattáneo et al. (Rodríguez-Cattáneo et al., 2013).

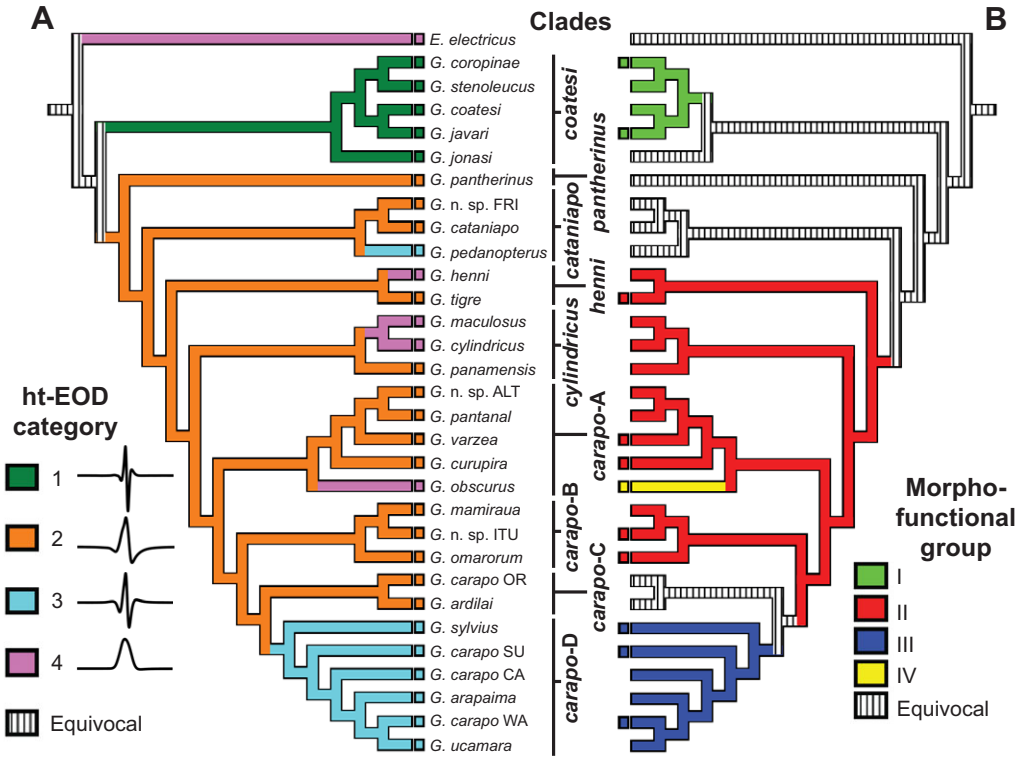

Fig. 1. Parsimony optimizations of (A) four head-to-tail electric organ discharge (ht-EOD) categories and (B) four morpho-functional groups, based on electric organ anatomy and electromotive force (emf)-EOD in *Gymnotus*. The phylogenetic tree is based on the Bayesian analysis of a four-gene data set (nuclear genes *rag2* and *zic1*; mitochondrial genes *16S rRNA* and *Cytochrome b*) for 30 *Gymnotus* species (Brochu, 2011). Species without ht-EOD data were pruned from the tree. Small boxes at tips of branches show states for each species; only 11 species have morpho-functional group data.

within the larger *G. carapo* clade with the labels '*G. carapo*-A clade' through '*G. carapo*-D clade' (Fig. 1).

Of relevance for the analyses described here is a change in position of *G. tigre* between Lovejoy et al. (Lovejoy et al., 2010) and Brochu (Brochu, 2011). In the former study, we sequenced immature individuals which have since been re-identified as *G. curupira*; in the latter study, we sequenced adult *G. tigre* specimens that were placed as the sister group of *G. henni*, matching the arrangement in the morphological phylogeny (Albert et al., 2005).

Outstanding issues include the placement of the southern Brazilian species *G. pantherinus*, whose precise sister group relationships have not yet been resolved. The systematics of *G. carapo* also requires additional study. Two species (*G. arapaima*, *G. ucamara*) described on morphological grounds as distinct from *G. carapo sensu stricto* [the species described by Linnaeus from Suriname, but apparently distributed across much of northern South America (see Albert and Crampton, 2003)] are nested within the clade corresponding to populations currently ascribed to *G. carapo sensu stricto*. This indicates that *G. carapo sensu stricto* may be a paraphyletic species within a rapidly diversifying complex of cryptic species (Albert et al., 2005; Lovejoy et al., 2010). Recent studies of the cytogenetics of species in the *G. carapo*-D clade have revealed morphologically indistinguishable forms with distinct chromosomal rearrangements (including changes in the diploid number), which are predicted to enforce post-zygotic reproductive isolation (Milhomem et al., 2008). For the purposes of this paper we report populations of *G. carapo* as independent taxonomic units, while for other species (in which we did not encounter similar taxonomic problems) we collapse populations into single terminals. In spite of these outstanding issues, we nonetheless regard the phylogeny of *Gymnotus* to be sufficiently well resolved to allow comparative analyses of EO and EOD evolution as described below.

Diversity, classification and phylogenetic distribution of ht-EODs

Most descriptions of gymnotiform and mormyriform EOD diversity characterize the EOD as the potential difference between two points, recorded as a head-to-tail EOD (ht-EOD) from electrodes located anterior to the head and posterior to the tail. ht-EOD recordings have the advantage that they can be readily obtained in the field from temporarily restrained fishes, and are easily quantified for cross-taxon comparisons. Moreover, there are grounds to consider the ht-EOD a reasonably faithful representation of the signal that one fish would detect from a conspecific at a distance of around one to two body lengths. Beyond one to two body lengths (but not close to a fish) the field generated by a fish resembles the unidirectional field generated by a simple dipole with an equivalent waveform (Hopkins, 2005; Knudsen, 1975), and can thus be approximated by the two-dimensional, time-voltage ht-EOD waveform. Moreover, Aguilera et al. (Aguilera et al., 2001) used a specially designed probe to record, at various locations on the skin of one fish (the receiver), the 'local conspecific field' cast onto it by another fish (a sender). They discovered that at the perioral electrosensory 'fovea' (the region of highest tuberous electroreceptor density and diversity), the local conspecific field recording closely resembled the far-field recorded ht-EOD of the sender (Aguilera et al., 2001) (see fig. 10 therein). Nonetheless, while the ht-EOD may serve as a readily quantifiable proxy of the signal than one fish detects from another, we stress that the electric field generated near a fish by its EOD exhibits much greater spatiotemporal complexity. This complexity results from the summing of the effects of multiple electrogenic units generating temporal waveforms, which are then modified by post-effector mechanisms (see 'The EOD as an effector act and the proximate mechanisms determining the EOD waveform' in the next section). The ht-EOD is therefore best regarded as a conveniently measurable epiphenomenon of a broader and more complex underlying set of

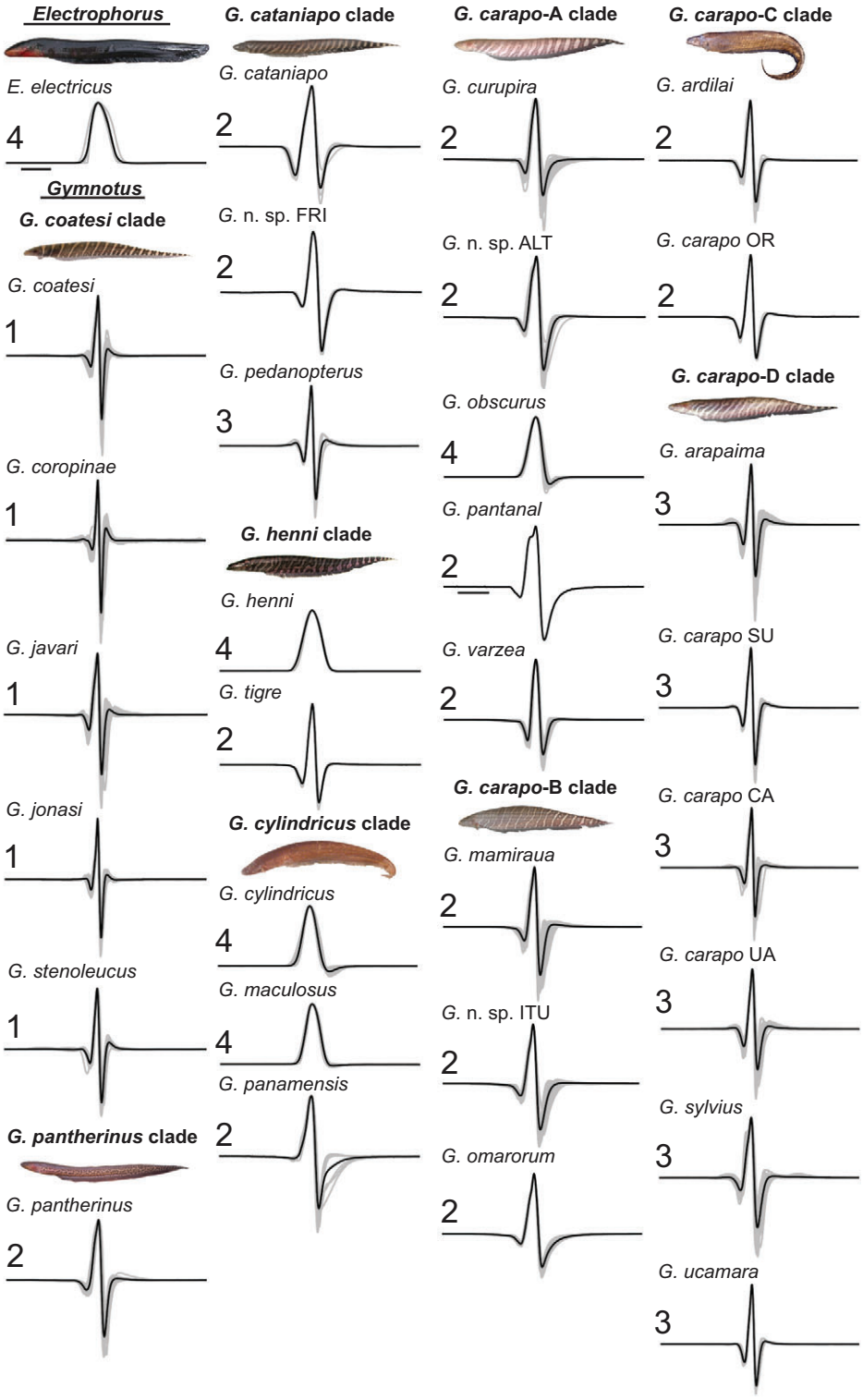

Fig. 2. ht-EOD waveforms of 30 species of *Gymnotus*, and *Electrophorus electricus*. Gray waveforms represent recordings of individual fishes (for sample sizes, see Table 2) and black waveforms represent the species averages. All waveforms are normalized to P_1 phase amplitude and plotted to the same time base (scale bar, 1 ms). ht-EOD category (1–4) is reported to the left of each waveform. Inset photographs are of *E. electricus*, *G. coatesi*, *G. pantherinus*, *G.* n. sp. FRI, *G. henni*, *G. maculosus*, *G. curupira*, *G. mamiraua*, *G. ardilai* and *G. arapaima*.

electrogenic mechanisms (the proximate bases of which we explore in the next section).

We conducted a comprehensive taxonomic survey of ht-EOD diversity in *Gymnotus*, based on expeditions through most of the geographical range of the genus, including Argentina, Bolivia, Brazil, Colombia, Costa Rica, Panama, Peru, Suriname, Uruguay and Venezuela. These expeditions yielded recordings of 1157 individual *Gymnotus* from 32 taxa (30 of which are included in our phylogenetic reconstruction), including 26 of the 37 described species in the genus, three as-yet-undescribed species, and three additional populations of *G. carapo* that are phylogenetically distinct from *G. carapo sensu stricto* (see Fig. 2, Table 2).

Our analyses show that *Gymnotus* taxa present from one to six components or 'phases' of alternating polarity in the ht-EOD waveform. Using a nomenclature which assumes that the dominant positive phase, P_1, is homologous among all *Gymnotus* (Crampton et al., 2008), the six phases are labeled sequentially: P_{-1}, P_0, P_1, P_2, P_3 and P_4. The equivalence to the EOD nomenclature that has been

Table 2. Head-to-tail EOD (ht-EOD) waveform structure and peak power frequency (PPF) metrics in *Gymnotus*

		Presence of phases						Phase amplitude						PPF (kHz)
Species/clade	*N*	P_{-1}	P_0	P_1	P_2	P_3	P_4	P_{-1}	P_0	P_1	P_2	P_3	P_4	Mean
***G. coatesi* clade**														
G. coatesi	66	0.304	1	1	1	1	0.304	0.027	–0.220	1	–1.132	0.142	–0.013	2.296
G. coropinae	153	0.980	1	1	1	1	0.536	0.026	–0.173	1	–1.271	0.247	–0.014	2.861
G. javari	137	0.080	1	1	1	0.993	0.218	0.024	–0.276	1	–1.031	0.123	–0.017	1.978
G. jonasi	97	0.680	1	1	1	0.979	0.546	0.033	–0.194	1	–1.001	0.100	–0.016	2.560
G. stenoleucus	14	0.500	1	1	1	1	0.143	0.020	–0.259	1	–0.939	0.129	–0.014	2.073
***G. pantherinus* clade**														
G. pantherinus	58		1	1	1	0.879			–0.175	1	–0.997	0.040		1.361
***G. cataniapo* clade**														
G. cataniapo	4		1	1	1	0.750			–0.493	1	–0.710	0.033		0.930
G. n. sp. FRI	2		1	1	1	1			–0.242	1	–1.021	0.050		1.120
G. pedanopterus	6	1	1	1	1	1		0.053	–0.288	1	–0.940	0.130		1.875
***G. henni* clade**														
G. henni	5			1						1				0.093
G. tigre	3		1	1	1	0.667			–0.316	1	–0.636	0.016		1.346
***G. cylindricus* clade**														
G. cylindricus	30			1	0.967					1	–0.028			0.123
G. maculosus	15			1	1					1	–0.094			0.181
G. panamensis	8		1	1	1	0.625			–0.043	1	–0.936	0.019		0.835
***G. carapo*-A clade**														
G. curupira	75		1	1	1	0.347			–0.257	1	–0.632	0.031		1.222
G. obscurus	23			1	1					1	–0.136			0.159
G. n. sp. ALT	20		1	1	1	0.950			–0.248	1	–0.909	0.026		1.107
G. pantanal	1		1	1	1				–0.172	1	–0.879			0.784
G. varzea	40		1	1	1	0.700			–0.367	1	–0.597	0.018		1.421
***G. carapo*-B clade**														
G. mamiraua	109		1	1	1	1			–0.254	1	–0.896	0.055		1.440
G. n. sp. ITU	43		1	1	1	0.651			–0.223	1	–0.810	0.032		1.079
G. omarorum	29		1	1	1				–0.173	1	–0.561			0.872
***G. carapo*-C clade**														
G. ardilai	12		1	1	1	1			–0.306	1	–0.749	0.026		1.559
G. carapo OR	2		1	1	1	1			–0.349	1	–0.695	0.059		1.434
***G. carapo*-D clade**														
G. arapaima	100	0.880	1	1	1	1		0.043	–0.358	1	–0.933	0.116		1.921
G. carapo SU	18	0.944	1	1	1	1		0.028	–0.317	1	–0.985	0.099		1.866
G. carapo CA	12	0.500	1	1	1	1		0.025	–0.326	1	–0.972	0.104		2.221
G. carapo WA	32	0.781	1	1	1	1		0.026	–0.316	1	–0.786	0.065		1.704
G. sylvius	36	0.333	1	1	1	1		0.027	–0.244	1	–0.936	0.043		1.330
G. ucamara	7	0.429	1	1	1	1		0.013	–0.326	1	–0.735	0.068		2.006

Presence of phases refers to the proportion of recorded individuals bearing each phase (with phases considered present in an individual if they exceed 1% of the P_1 amplitude). Phase amplitude values are reported as proportions of the P_1 amplitude, which was normalized to 1.

See 'Diversity, classification and phylogenetic distribution of ht-EODs' for description of phases. All recordings are from intact specimens, including large juveniles, immature adults and sexually mature males and females [see Crampton et al. (Crampton et al., 2011) for definition of growth stages].

used to characterize the electromotive force EOD (emf-EOD) through recordings of fish suspended in air (see 'Interspecific diversity in the EO and emf-EOD' in the next section) is approximately: $P_0=V_1+V_2$, $P_1=V_3$, $P_2=V_4$, $P_3=V_5$, $P_4=V_6$ (Rodríguez-Cattaneo et al., 2008) (with V_6 added here). Nonetheless, the order of peaks in the ht-EOD neither necessarily reflects equivalent spatial origin nor similar generation mechanisms, and therefore the 'P' nomenclature for the ht-EOD and the 'V' nomenclature for the emf-EOD do not always match. For instance, a weak positive P_{-1} phase in *G. carapo* SU is the result of a slow positive wave from the central and tail regions' V_{1ct} overcoming a simultaneous V_{1r} of opposite polarity, while in *G. coropinae* P_{-1} is generated by V_{3r} in the tail region (subscripts r, c and t signify rostral, central and tail [caudal], respectively) (Rodríguez-Cattaneo et al., 2008).

Table 2 reports the average voltage for each of the six ht-EOD phases P_{-1} through P_4, and also the proportion of all recorded individuals that exhibit each of these six phases. For a phase to be recognized in a given individual, the voltage had to exceed a 1% threshold of the voltage of the P_1 phase. The 1% threshold was chosen because it lies above recording noise, while capturing weak but valid phases of morpho-functional importance.

To interpret ht-EODs using evolutionary analyses, waveform structure needs to be categorized into hypothesized homologous categories (character states). However, determining appropriate character states presents two challenges. First, simply categorizing waveforms by number of phases (Lovejoy et al., 2010) may oversimplify underlying variation; for example, in two taxa with four distinct phases, one might exhibit P_{-1}, P_0, P_1 and P_2, while the other could exhibit P_0, P_1, P_2 and P_3. Therefore, we categorized ht-EOD structure based on which specific phases were represented in the waveform. Second, at the low thresholds necessary to recognize weak phases, ht-EOD phases are often polymorphic among individuals from a given species or population. This especially becomes a problem for the weak flanking phases P_{-1}, P_3 and P_4. To accommodate polymorphism while simplifying the coding of ht-EOD structure, we defined phases as being 'present' if represented by ≥97% of recorded individuals and 'polymorphic' if present in >0 to <97% of recorded individuals. Based on this scheme, and on the peak power frequency (PPF) in the power spectral density of the ht-EOD, we defined four types of ht-EOD structure (named arbitrarily), which are listed in Fig. 2 (left of the ht-EOD for each taxon) and Table 2, and described in detail below.

Category 1 (>4 phases, with P_4 present): here four phases are always present (always $P_0+P_1+P_2+P_3$), a fifth phase (P_4) is expressed polymorphically, and a very weak sixth phase (P_{-1}) is either present or expressed polymorphically. Mean PPFs are high, ranging from 1.978 to 2.861 kHz.

Category 2 (3–4 phases): three phases are always present (always $P_0+P_1+P_2$), with a fourth phase (always P_3) either present, expressed polymorphically or absent. Mean PPFs are intermediate, ranging from 0.784 to 1.421 kHz.

Category 3 (>4 phases, with P_4 absent): four phases are always present (always $P_0+P_1+P_2+P_3$), and a fifth phase (always P_{-1}) is expressed polymorphically. This category differs only slightly from category 1 in that P_4 is never present. Mean PPFs are intermediate to high, ranging from 1.330 to 2.221 kHz (if *G. sylvius* is excluded the range is 1.704–2.221 kHz).

Category 4 (1–2 phases): P_1 is always present, P_2 is either present, expressed polymorphically or absent, and all other phases are always absent. Mean PPFs are very low, ranging from 0.093 to 0.181 kHz. In this group, P_2 never exceeds 26.5% of the P_1 voltage; unlike in the Hypopomidae there are no purely biphasic species of *Gymnotus* in which P_2 approximately matches P_1 in amplitude [many specimens of *G. panamensis* approximate this kind of waveform (see Fig. 2), but in this species a weak P_0 is present and a weak P_3 is expressed polymorphically]. For brevity, we henceforth refer to the quasi-monophasic and monophasic conditions observed in ht-EOD category 4 as simply 'quasi-monophasic'.

To explore the evolution of ht-EOD structure, we used parsimony-based optimization to map these four ht-EOD character states onto the molecular phylogenetic reconstruction of *Gymnotus* described above (see Fig. 1A). This procedure reconstructs the character condition for each branch in the tree, allowing us to hypothesize transitions in EOD structure during the diversification of the genus. Our analyses reveal a basal dichotomy between the *G. coatesi* clade, in which the ancestral condition is ht-EOD category 1 (4+ phases with high PPF), and the clade comprising all remaining *Gymnotus* species, in which the ancestral condition is ht-EOD category 2 (3–4 phases with intermediate PPF).

Within the larger clade comprising the *G. pantherinus*, *G. cataniapo*, *G. henni*, *G. cylindricus* and *G. carapo* clades, there are two independent transitions from ht-EOD category 2 to 3 (which involves the appearance of P_{-1} and an elevation of the PPF): once in the *G. carapo*-D clade, and once in *G. pedanopterus* (*G. cataniapo* clade). Finally, within *Gymnotus*, there are three independent transitions from ht-EOD category 2 to the quasi-monophasic condition of ht-EOD category 4, in each case involving the loss of P_0 and P_3, and the partial or complete loss of P_2: once in *G. henni* (*G. henni* clade), once in the ancestor of *G. cylindricus* + *G. maculosus* (*G. cylindricus* clade), and once in *G. obscurus* (*G. carapo*-A clade). The sister taxon to *Gymnotus*, *Electrophorus electricus*, also has a category 4 ht-EOD, but this is generated from highly specialized electric organs that generate both weak discharges for electrolocation and strong (to ca. 550 V) discharges for stunning prey and for defense (Crampton and Albert, 2006).

Proximate causes of EOD diversity in *Gymnotus*

The EOD as an effector act and the proximate mechanisms determining the EOD waveform

Electric fields resulting from EODs are generated as a continuous train of pulses from a myogenic hypaxial EO located along most of the length of the body, and detected by an array of cutaneous electroreceptors. Changes in the transcutaneous pattern of the self-generated electric field inform the fish about the presence and attributes of nearby objects (electrolocation). Likewise, changes in the transcutaneous pattern of allo-generated electric fields also inform *Gymnotus* about the presence of neighboring electric fish, mediating communication and possibly recognition.

The EOD can be considered at the organismal level of integration as an 'effector act' resulting from the convolution of a series of impulses with a spatiotemporal pattern of EO activation. As long as the pacemaker activity remains within a resting range (typically between 15 and 70 EODs s^{-1}), the pattern of activation is stereotyped. It is essential to emphasize that, unlike in mormyrids, the electric field generated by the EOD of gymnotiforms is the sum of the effects of multiple electrogenic units, each generating a specific temporal waveform along the EO, which are then weighted by post-effector mechanisms of current summation along the fish's body to produce the characteristic field in the water. The most important post-effector mechanisms involve current funneling, which is determined by the shape and conductance of tissues surrounding the EO.

Recent studies have demonstrated that the multiple current sources along the EO of pulse gymnotiforms do not all perform the same roles in electrolocation and communication, and are far from uniformly represented in the ht-EOD (Aguilera et al., 2001; Caputi and Nogueira, 2012; Rodríguez-Cattáneo et al., 2008). On the contrary, it is now clear that the rostral region of the body generates a relatively low-frequency field with a constant waveform that is oriented perpendicular to the skin, and is much stronger than elsewhere on the fish's surface. This rostral field is funneled into the region near the fish's mouth and effectively serves to 'illuminate' the perioral electrosensory fovea of highest tuberous electroreceptor density and type variety, where the electrosensory array has its highest resolution (Castelló et al., 2000). The rostral field is therefore considered the main carrier of active electrolocation. In contrast, the central and caudal portions of the body contribute higher voltage and higher frequency components to the EOD field, which – because of the greater length of the dipole and the higher internal resistance of the equivalent source – extend further from the body. These central and caudally generated components exhibit wide variation among species (Rodríguez-Cattáneo et al., 2008) and appear to serve primarily for communication. In sum, the EOD exhibits a spatiotemporal complexity that is important for both the specificity of the reception and the separation of the two signal carriers according to their function: one used primarily for active electrolocation, and the other for electrocommunication (Aguilera et al., 2001).

Biophysical analysis of the electric field generation indicates that actively generated electric images of objects, and passively received signals from other fish, can be modeled by considering the fish body as a distributed source. This source can typically be characterized as a spatiotemporal pattern of the electromotive force (referred to here as the emf-EOD, see 'Interspecific diversity in the EO and emf-EOD' for definition) and an internal load [see 'Thevenin theorem' in Donaldson (Donaldson, 1958)]. The emf-EOD is the consequence of the coordinated activation of different types of electrogenic units at specific locations along the EO, with specific timings, and whose individual contribution to the whole EOD is differently weighted by the surrounding tissue.

The immediate proximate cause of the external electric field is the asymmetric activation of an electrocyte membrane (Albe-Fessard and Chagas, 1954; Albe-Fessard and Chagas, 1955; Altamirano et al., 1953; Bennett and Grundfest, 1959). This causes a loss of the electric equilibrium of the cell membrane and the flow of currents through the surrounding tissues. To generate a significant external field, membrane patches that are equally oriented in space must be activated synchronously; this vital coordination task that the nervous system has to perform is found in both gymnotiforms and mormyriforms (Bennett, 1971).

The activation of equally oriented membrane patches is the proximate mechanism determining every EOD component generated by the myogenic electrocytes. However, synchronous recruitment of equally oriented membrane patches may occur in three situations (Fig. 3): activation mechanism 1, when the neural drive provokes end plate potentials at the electrogenic membranes (Lorenzo et al., 1988); activation mechanism 2, when the neural drive provokes action potentials at the electrogenic membranes (Bennett and Grundfest, 1959; Macadar et al., 1989); and activation mechanism 3, when the action currents generated by the same or neighboring electrocytes depolarize the oppositely oriented membrane patch (auto-excitation) (Macadar et al., 1989; Rodríguez-Cattáneo and Caputi, 2009).

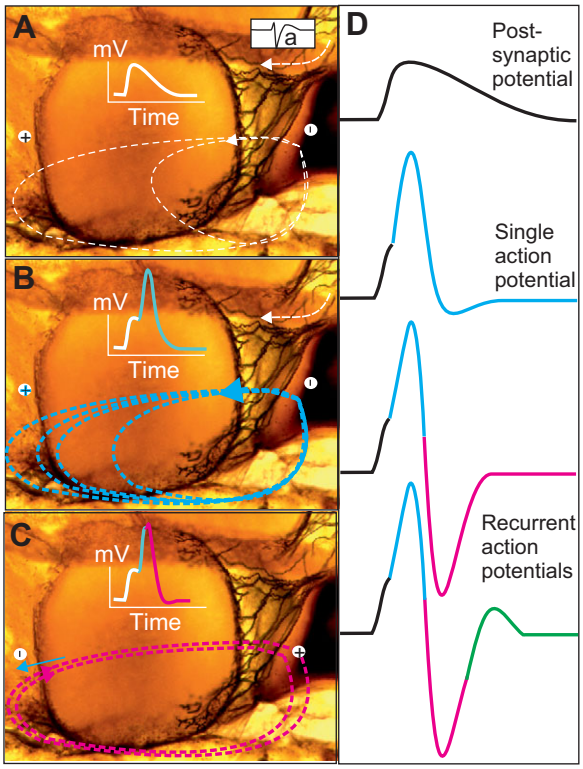

Fig. 3. Activation mechanisms of electrocyte membranes and their relation to EOD waveform in *Gymnotus*. (A) Action potentials coming through electromotor neuron axons (arrow and box) elicit post-synaptic potentials on the innervated face (plot inside the electrocyte). This generates smooth waves in the electric field (white traces on the photograph and black traces in D). (B) If the membrane is excitable and the depolarization suffices, an action potential is generated, causing a sharper and larger deflection in the electric field (cyan traces schematize the current flow, the action potential and the waveform component). (C) If both opposite faces are excitable, action potentials can be propagated – causing a biphasic waveform (represented in magenta). (D) Schematics of the four types of waveforms that can be achieved by variations of the responsiveness of the electrocyte to a single nerve volley. The bottom trace illustrates that a third wave (represented in green) can be generated if some electrocytes show enough excitability. Insets inside the electrocyte images schematize the time course of intracellular potential. The origin of current flow to each component is color coded as in D.

In mechanisms 1 and 2 above, activation is necessarily linked to an elementary component of the EOD, and in the simplest cases leads to monophasic EODs, for example in *Electrophorus* (Albe-Fessard and Martins-Ferreira, 1953) (reviewed in Bennett, 1971). *Gymnotus obscurus* and *G. pantanal* exhibit clear examples of monophasic discharges at the rostral regions of the EO (Fig. 4). Paccini's principle states that the innervated electrocyte face becomes negative during neural activation (Grundfest, 1961). Differences in amplitude and duration of the discharge depend on the channel repertoire exhibited by the membrane (Markham et al., 2009; Markham and Stoddard, 2005; Sierra et al., 2007; Sierra et al., 2005). Auto-excitation is a means of generating more than one wave component (i.e. phase) after a single neural command, thereby alternating the polarity of the discharge. This is characteristic of mormyrids (Bennett, 1971; Hopkins, 1999a), but is also common in pulse gymnotiforms, with direct evidence from *Gymnotus*, including *G.* sp. misidentified as *G. carapo* (Bennett and Grundfest, 1959) and *G. omarorum* (Macadar et al., 1989), and

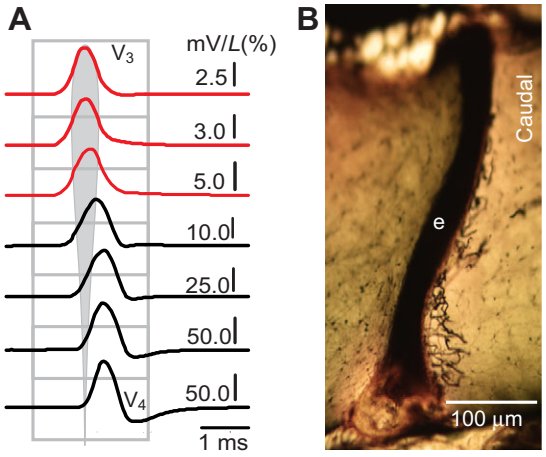

Fig. 4. Monophasic activation in *Gymnotus obscurus*. (A) Spatiotemporal pattern of electromotive force. Vertical bars for mV/*L*(%) represent amplitude in mV as a function of the generator position – i.e. distance from snout expressed as a percentage of total length (*L*). Red traces obtained from rostral regions indicate the lack of responsiveness of the rostral faces of the electrocytes. (B) A monoinnervated electrocyte (marked e) from the central region of the fish's body.

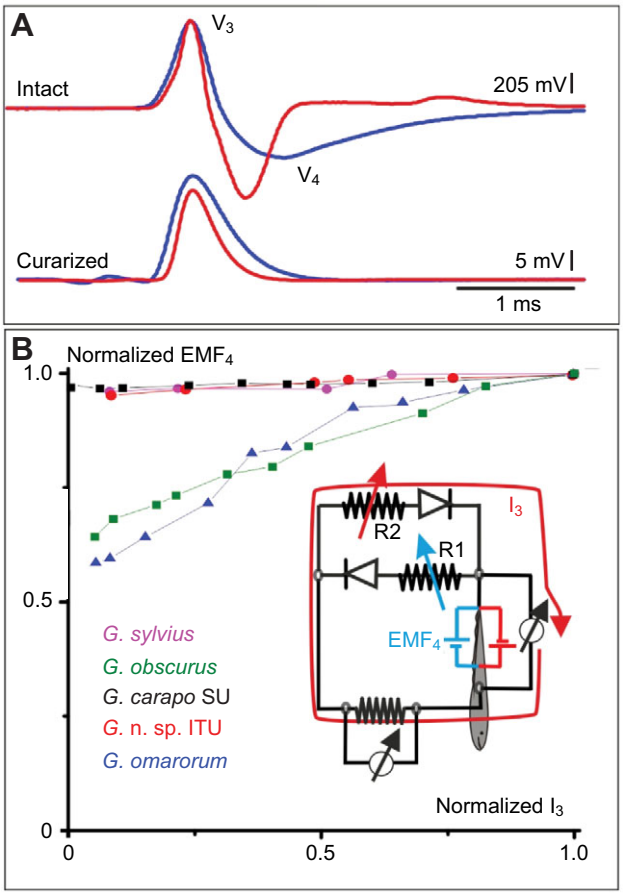

Fig. 5. Electric organs can be differentiated by their auto-excitability. (A) Differences in the EOD generated at the tail region between two closely related species: *Gymnotus omarorum* (blue), with a wide V_4, and *G.* n. sp. ITU, with a sharp V_4 and a positive V_5. The late components generated by the electrocyte responsiveness to a single volley can be eliminated by curarization. (B) The excitability can be explored by analyzing the electromotive force generated by the rostral faces (EMF_4, blue battery) as a function of the external current associated with the activation of the caudal faces (I_3, red battery). While *G. obscurus* (morpho-functional group IV) and *G. omarorum* (group II) require the circulation of external current to maximize V_4, *G. coropinae* (group I), *G.* n. sp. ITU (group II), *G. carapo* SU, *G. carapo* WA and *G. sylvius* (Group III) do not. The technique is schematized in the inset (for details, see Rodríguez-Cattáneo and Caputi, 2009).

Brachyhypopomus (Hagedorn and Carr, 1985; Markham and Stoddard, 2005), and with indirect evidence from *Rhamphichthys* (Caputi et al., 1994). It is important to note that: first, the initial deflection of the EOD waveform cannot result from auto-excitation; second, the timing between the neurally activated component and the secondary component is determined by the geometry and intrinsic properties of the electrocyte; and third, reduction of the synaptic potential by partial curarization may lead to a reduction of the auto-exciting current below the threshold of the opposite membrane (Fig. 5). This last procedure, when applied to an intact fish, may diagnose the neural or local origin of a wave component (Caputi et al., 1989). Furthermore, auto-excitation currents may be enforced by adding a directional external load when they are insufficient to cause the recruitment of all opposite membrane faces (Bell et al., 1976; Caputi et al., 1998; Rodríguez-Cattáneo and Caputi, 2009). Therefore, this procedure allows one to quantify the auto-excitability of the EO in an intact fish (Rodríguez-Cattáneo and Caputi, 2009) (Fig. 5).

Auto-excitation is not the only way to generate multiple EOD phases. Some electrocytes of *Gymnotus* (Szabo, 1961; Trujillo-Cenóz and Echagüe, 1989) and *Rhamphichthys* (Caputi et al., 1994; Trujillo-Cenóz et al., 1984) are double innervated. In these double innervated electrocytes, a precise succession of the neural commands activating each face determines the activation of opposite faces, and also sets the timing between successive components. The precise synchronism required to summate equally oriented faces, and the activation sequencing required to determine the timing between neutrally activated components, is achieved by the presence of a combination of central and peripheral delay lines (Bennett, 1971; Caputi and Aguilera, 1996; Lorenzo et al., 1990; Lorenzo et al., 1993), and by the presence of different electromotor neuron pools innervating variably oriented electrocyte faces (Caputi and Trujillo-Cenóz, 1994). In sum, important proximate causes of complexity in the electric field of *Gymnotus* (and also *Rhamphichthys*) are the heterogeneous distribution of the electrocyte types along the EO and the role of a central pattern generator in yielding the proper sequence of activation (Caputi and Aguilera, 1996; Caputi et al., 1994; Trujillo-Cenóz and Echagüe, 1989) (Fig. 6).

In general, the more rostral regions of the EO, including the abdominal and sometimes the head region, as is the case in *G. javari* and *G. coropinae* (see below), exhibit the lowest electrocyte density and the largest diversity of electrogenic mechanisms – including activation mechanisms 1–3 listed above – and in the case of *G. javari* and *G. coropinae*, some electrocytes penetrating the head also show complex geometry (Castelló et al., 2009) (Fig. 7). In contrast, the caudal portion of the EO shows monotonically tightly packed, caudally innervated electrocytes that generate one to three phases, depending on the auto-excitability typical of the species (Castelló et al., 2009; Rodríguez-Cattáneo and Caputi, 2009; Rodríguez-Cattáneo et al., 2008; Rodríguez-Cattáneo et al., 2013; Trujillo-Cenóz and Echagüe, 1989). The central portion of the EO exhibits electrocyte properties intermediate between those of the rostral and caudal portions.

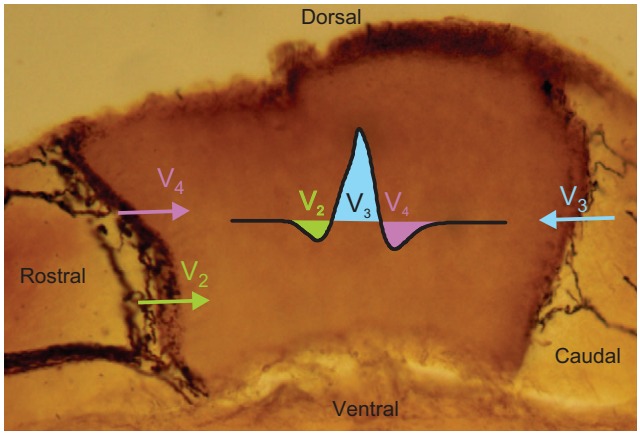

Fig. 6. A typical feature of *Gymnotus* is the presence of double innervated electrocytes. The sequential neural activation of opposite faces gives origin to the sequence V_2 (green)–V_3 (cyan). The triphasic pattern is completed by the 'invasion' of the rostral face by the action potential generated at the caudal face (magenta).

Finally, the relatively low conductivity of the non-electrogenic tissues and the shape of the fish's body together constitute a heterogeneous external load to the EO. These parameters act as a weighting factor for the contributions of individual electrogenic units, which cause the electromotive force pattern when summated. In addition, fish conductance is a post-effector mechanism that determines the partitioning of currents between the inside of the body and the water.

In light of the considerations above, to elucidate the proximate mechanisms of signal diversity it is necessary to determine the differences between electrocyte types, their patterns of activation and control mechanisms, and the location and membrane orientation of the different electrocyte types within the body structure. These heritable characters span different levels of integration, including the molecular level (electrocyte membrane channel repertoire), the cellular level (the discharge of a single electrocyte as a unit), a circuital level (the innervation pattern of the electrocytes, the electromotor neurons and the EO as a whole), a broader functional level (as a neural network, or as EO activation patterns) and finally the organismal level (here the body shape conditions current flow through the passive tissues, providing different weights and possibly functional roles to the currents generated by individual electrocytes). Below, we describe a comparative survey of the proximate causes of electric signal diversity in *Gymnotus* and conclude that the differential expression of a small number of these characters underlies the proximate basis of EOD diversity.

Interspecific diversity in the EO and emf-EOD

We conducted a detailed survey of the morpho-functional basis of signal diversity, with emphasis on cellular- and organismal-level variation in EO anatomy and the emf-EOD, for 11 species, including representatives of as many clades of *Gymnotus* as we could obtain for laboratory study. These were: *G. omarorum* from a coastal drainage of Uruguay, *G. carapo* SU and *G. coropinae* from coastal drainages of Suriname (Castelló et al., 2009; Rodríguez-Cattáneo et al., 2008), *G.* n. sp. ITU from the Paraná drainage (Rodríguez-Cattáneo and Caputi, 2009), *G. sylvius* from the Paraná drainage, and *G. carapo* WA, *G. curupira*, *G. javari*, *G. obscurus*, *G. tigre* and *G. varzea* from the Peruvian Amazon (Rodríguez-Cattáneo et al., 2013).

To characterize the spatial complexity of the EOD along a fish's body, free of the effect of conductivity (due to the spatial variation of electromotive force and the series resistance of the fish body's equivalent source, the field generated in water, including the ht-EOD, is sensitive to conductivity), we employ two methodological approaches. First, we characterize the emf-EOD – that is, the electromotive force pattern of the EOD generated in the absence of external load – by suspending the fish in air. We acknowledge that in some cases the emf-EOD itself is load-dependent, but this can be characterized instrumentally (Bell et al., 1976; Caputi et al., 1998; Rodríguez-Cattáneo and Caputi, 2009). Second, we characterize the internal load of the fish's body, which depends mainly on the mean conductivity and shape of the fish itself. The approaches we used in the morpho-functional survey are based on concepts and methodologies developed from a long and detailed

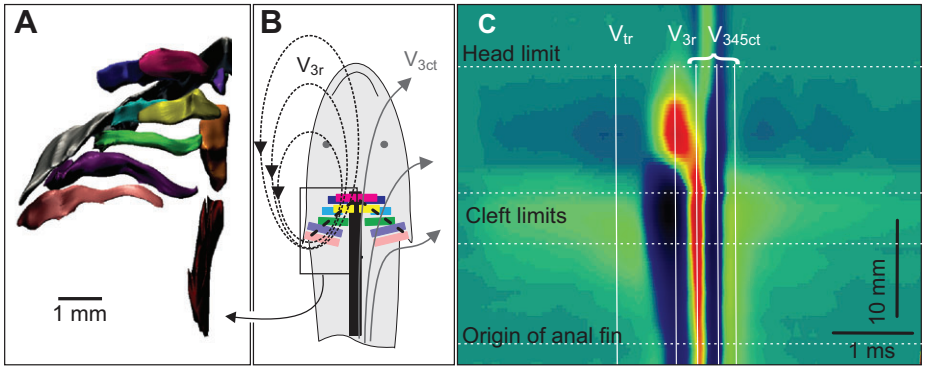

Fig. 7. Species in the *G. coatesi* clade exhibit an expansion of the electric organ (EO) into the head. (A) Ventral view of a 3D reconstruction of this portion of the EO in *G. coropinae*, illustrating the position of seven large electrocytes, which constitute a lateral part of this expansion on each side of the body. (B) Schematic of the arrangement of these seven electrocytes along the cleithral aponeuroses (bold dotted line). Note that four of the electrocytes (shown in red, blue, cyan and yellow) invade the head below the cleithral aponeuroses. (C) The expansion of the EO into the head gives origin to early waves that precede the main discharge of the EO. The color map shows the transcutaneous current flow along a horizontal line during the discharge. The activation of the rostral expansion starts very early (blue sink and lime-green source reaching a maximum at the V_{1r} line). Following this component, a head-positive (red source–blue sink) occurs at the V_{3r} line. This corresponds to the dotted black current lines schematized to the left. Later, the main discharge is activated (V_{345ct}) generating, at V_{3ct}, the flow of currents schematized with gray lines.

series of studies involving cellular and whole-organism integrative analysis in the model species *G. omarorum*.

Our analyses yielded a classification of *Gymnotus* into four morpho-functional groups, which we name, arbitrarily, groups I through IV, using Roman numerals to discriminate from the Arabic numbers used for the ht-EOD categories.

Morpho-functional group I

Two species, *G. coropinae* (Castelló et al., 2009; Rodríguez-Cattáneo et al., 2008) and *G. javari* (Rodríguez-Cattáneo et al., 2013), generate a low-power EOD with a complex near field. Unlike all other *Gymnotus* species, these exhibit an expansion of electrogenic tissue of the EO into the head, in the area of the pelvic girdle posterior and ventral to the cleithral aponeurotic sheath (Castelló et al., 2009) (Fig. 7). This feature results in a slow rostral EOD component with a power spectrum peaking at relatively low frequencies and comprising a head-negative V_{1r} peak followed by a head-positive peak (V_{3r}, corresponding to P_{-1} in the ht-EOD). Double innervated electrodes in the central and caudal regions of the EO generate a sharp multiphasic component comprising a $V_{2–3–4–5}$ (P_0–P_3) sequence with peak power at high frequency ranges, and a clearly defined V_5 (P_3). This corresponds to a high mean PPF in the ht-EOD (>1.9 kHz). The low amplitude of EODs in this clade is likely the consequence of a substantially lower electrocyte density than in other *Gymnotus* species (with a characteristic electrocyte elongation) and/or because the duration of each EOD component is much shorter than a usual action potential, implying a larger degree of overlap between the action potential generated by opposite faces. Also, low amplitude is likely, in part, a consequence of small body size; this is the subject of ongoing work.

Morpho-functional group II

This group, comprising *G. tigre*, *G. curupira*, *G.* n. sp. ITU, *G. omarorum* and *G. varzea*, has EODs that begin with a smooth negative component generated at the abdominal region by the activation of the rostral faces of double innervated electrocytes (V_{1r}), followed by a complex $V_{2–3–4}$ (≈P_0–P_2) pattern generated at the central region, with the major positive peak (P_1=V_3) resulting from the activation of the caudal faces of single innervated electrocytes. Interspecific variation in the ht-EOD waveforms mainly depends on the extent to which the rostral face of the electrocytes is auto-excitable. For instance, *G. curupira* and *G.* sp. ITU exhibit the largest auto-excitability, show the largest and sharpest V_4, and may also show a small late positive component, V_5 (P_3) (Fig. 5). At the other extreme, *G. omarorum* shows low auto-excitability and generates a very small V_4 (P_2) (Fig. 5). Between these extremes we observe intermediate amounts of auto-excitability, and intermediate V_4 parameters (see Table 3, Fig. 8C). V_4 is expected to exhibit variation with temperature and sexual differentiation, due to the plastic nature of auto-excitability (Caputi et al., 1998). For instance, this may explain the sexually dimorphic nature of the V_4 (P_2) and V_5 (P_3) components of the ht-EOD of *G. curupira* (Crampton et al., 2011) (see below). Nonetheless, we have observed species-level variation in auto-excitability, independent of sex and season, between *G.* n. sp. ITU and *G. omarorum* (Rodríguez-Cattáneo and Caputi, 2009) (Fig. 5).

Morpho-functional group III

This group comprises *G. carapo* SU, *G. carapo* WA and *G. sylvius*. As in functional group II, a characteristic slow negative early component of the EOD is generated in the abdominal region by the activation of double innervated electrocytes, and the following positive peak from the activation of the caudal face of single innervated electrocytes. This group is also characterized by the presence of an earlier positive slow wave at the head-to-tail electric field (V_{1ct}) which is responsible for the P_{-1} variably present in the ht-EOD (its expression is dependent partially on temperature and conductivity). Unlike in functional group I (where the P_{-1} phase corresponds to V_{3r}, generated in the rostral region), the caudally generated P_1 (V_{1ct}) phase in functional group III is likely of neural origin – originating from the large posterior electromotor nerve, the synchronic activation of which occurs at the same time that abdominal electrocytes are

Table 3. Salient morpho-functional factors determining interspecific signal diversity in *Gymnotus*

		Cellular level			Organismal level	
Functional group	Species	Innervation pattern of the electrocyte	Autoexcitability	Neurally generated components in htEOD	Distribution of electrocyte types	Electrocyte density
–	*Electrophorus*	Monoinnervated electrocytes **(3)**	Very low **(1)**	Unknown	Not applicable	Unknown
I	*G. coropinae* *G. javari*	Double innervated electrocytes generating V_2–V_3 pattern **(1)**	High **(4)**	No **(1)**	4 distinct regions of EO (with one extending into the head below the cleithrum) **(1)**	Low **(1)**
II	*G. curupira* *G.* n. sp. ITU *G. omarorum* *G. tigre* *G. varzea*	Double innervated electrocytes generating V_1–V_3 pattern at the abdominal region and V_2–V_3 pattern at the central region **(2)**	Intermediate **(3)** High **(4)** Low **(2)** Intermediate **(3)** Intermediate **(3)**	No **(1)**	3 distinct regions of EO **(2)**	High **(2)**
III	*G. carapo* WA *G. carapo* SU *G. sylvius*	Double innervated electrocytes generating V_1–V_3 pattern at the abdominal region and V_2–V_3 pattern at the central region **(2)**	High **(4)**	Yes **(2)**	3 distinct regions of EO **(2)**	High **(2)**
IV	*G. obscurus*	Monoinnervated electrocytes **(3)**	Very low **(1)**	No **(1)**	Unknown	Unknown

Character states (in bold) refer to Fig. 8.

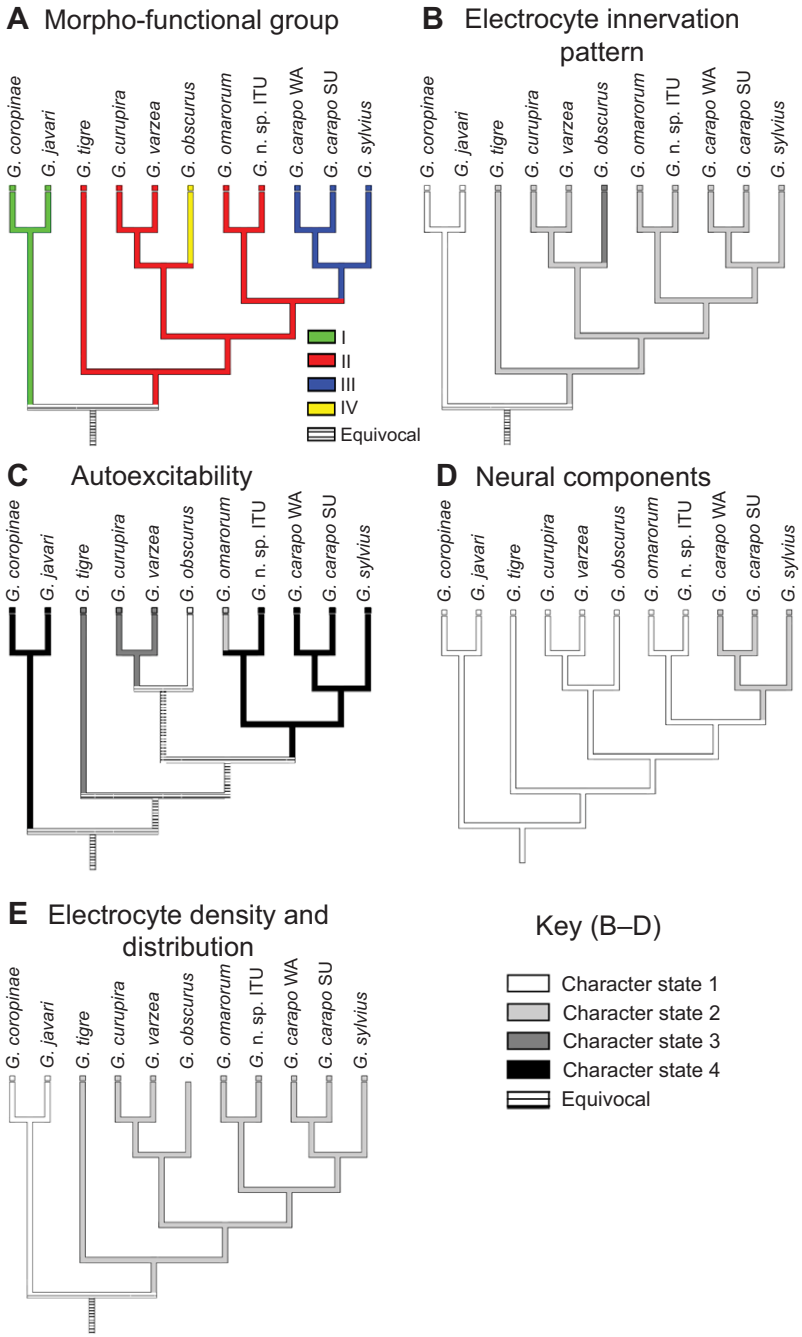

Fig. 8. Parsimony optimizations of cellular- and organismal-level aspects of the EO and emf-EOD in *Gymnotus*. Character states are from Table 3. Phylogenetic tree as per Fig. 1; species that have not yet been characterized were pruned. Small boxes at tips of branches show states for each species. Note: the two characters in D have identical state distributions among species and identical optimizations.

responding to the synaptic volley with an end plate potential. Neurally generated components detectable in the ht-EOD are never present in *Gymnotus* species from other morpho-functional groups. Species in functional group III, as in some members of group II, exhibit high auto-excitability of the electrocytes, manifested by the sharpness and load-independence of V_4, and the presence of V_5.

Morpho-functional group IV

This group is represented by one species, *G. obscurus*. The EOD of *G. obscurus* is quasi-monophasic, beginning with the main positive wave V_3 (P_1) and followed by a small, load-dependent second phase V_4 (P_2) that occurs at the tail region (Fig. 4). All other EOD components are absent. The electromotive force of V_4 is highly dependent on the amount of longitudinal current associated with V_3. Rostral innervations appear to be absent in all of the electrocytes in *G. obscurus*, all of which are disc shaped.

The phylogenetic distribution of morpho-functional groups and their correspondence to ht-EOD categories

In this section we discuss the phylogenetic (and also geographical and ecological) distribution of the four morpho-functional groups defined above, and their correspondence to the categories of ht-EODs described above (in ‘Diversity, classification and phylogenetic distribution of ht-EODs’). Here we refer the reader to Fig. 1, which shows the phylogenetic distribution of ht-EOD categories 1–4 and morpho-functional groups I–IV for 30 taxa, and to Fig. 8A, which shows the phylogenetic distribution of functional groups on a reduced tree (representing only the 11 species for which we compiled morpho-functional data).

Fig. 8B–D also illustrates the phylogenetic distribution of five salient characters underlying signal diversity, which are summarized in Table 3.

Morpho-functional group I

Morpho-functional group I corresponds to two species in the *G. coatesi* clade: *G. coropinae* and *G. javari*. Three additional species in the same clade, for which detailed studies of the EO anatomy and emf-EOD have not yet been conducted (*G. coatesi*, *G. stenoleucus* and *G. jonasi*) exhibit very similar, category 1 ht-EODs and likely share similar proximate bases for the EOD, including the unusual extension of the EO into the head. Likewise, character mapping of the four functional group states (Fig. 1B) optimizes the clade comprising (*G. coropinae* + *G. stenoleucus*) + (*G. coatesi* + *G. javari*) to functional group I, leaving only *G. jonasi* equivocal. We expect that functional data for *G. jonasi*, when available, will most likely optimize the entire *G. coatesi* clade to functional group I, yielding a precise correspondence between functional group I and ht-EOD category 1.

Category 1 ht-EODs exhibit mean PPFs exceeding 1.9 kHz, the presence of a very weak terminal negative P_4 (V_6) phase, and the variable presence of an early positive P_{-1} phase corresponding to V_{3r}. Species in the *G. coatesi* clade are similar in morphology, with a slender shape and small body size, reaching a maximum total length of 240 mm (with some species, e.g. *G. coropinae*, maturing at as little as 80 mm). Members of the clade are restricted to tropical systems, reaching latitudes of ~6°N and 12°S, and occur in both low-conductivity (5–30 μS cm^{-1}) (*G. coatesi*, *G. coropinae*, *G. javari* and *G. stenoleucus*) and high-conductivity (100–250 μS cm^{-1}) systems (*G. jonasi*, *G. melanopleura* and *G. onca*) (Table 1).

Morpho-functional group II

The species we assigned to this group (*G. tigre* in the *G. henni* clade, and *G. curupira*, *G.* n. sp. ITU, *G. omarorum* and *G. varzea* in the *G. carapo* clade) all exhibit category 2 ht-EODs, in which phases P_0–P_2 ($V_{1–4}$) are always present, and a fourth phase P_3 (V_5) is either present, absent or polymorphically present. Variation in ht-EOD waveform within this functional group – especially the relative amplitude of V_4 and the presence of V_5 – is largely the result of variation in auto-excitability (see Fig. 5).

Character mapping (Fig. 1B) optimizes functional group II to a paraphyletic grouping comprising the *G. henni* clade, the *G. cylindricus* clade, the *G. carapo*-A clade (excepting *G. obscurus*, which has undergone a transition to the functional group IV condition) and the *G. carapo*-B clade. As we discuss below, this optimization is likely in error with respect to *G. henni*, and *G. cylindricus* + *G. maculosus*, all of which possess quasi-monophasic category 4 ht-EODs.

Excepting *G. henni*, *G. cylindricus*, *G. maculosus* and *G. obscurus*, all species within the group optimized to functional group II generate category 2 ht-EODs (note the perfect correspondence between red branches in Fig. 1B and orange branches in Fig. 1A). We hypothesize that this optimization into functional group II is likely accurate for the following species for which we recorded ht-EODS but did not conduct anatomical and emf-EOD analyses: *G. panamensis*, *G.* n. sp. ALT, *G. pantanal* and *G. mamiraua*. Based on the presence of category 2 ht-EODs in *G. carapo* OR and *G. ardilai*, we speculate that the *G. carapo*-C clade (currently optimized as equivocal) may also belong to functional group II.

Because we did not conduct detailed anatomical and emf-EOD analyses for *G. pantherinus*, or any species in the *G. cataniapo* clade, the basal part of the large clade forming the sister taxon to the *G. coatesi* group cannot be optimized to any functional group (equivocal in Fig. 1B). Nonetheless, given that *G. pantherinus* and two members of the *G. cataniapo* clade (*G. cataniapo* and *G.* n. sp. FRI) exhibit the ht-EOD category 2 (shared with most other species in functional group II), we speculate that the ancestral condition in the sister taxon to the *G. coatesi* clade is functional group II. As such, we postulate that early in *Gymnotus* evolution there was a divergence between functional group I (in the *G. coatesi* clade) and functional group II (in the large sister clade to *G. coatesi*). Unfortunately, because the highly specialized electrogenic system of *Electrophorus* precludes comparisons to the functional groups in *Gymnotus*, we are unable to deduce which (if either) of functional groups I or II represents the ancestral condition at the base of *Gymnotus*. Nevertheless, we can deduce that the ancestral condition in *Gymnotus* is double innervation of the electrocytes, yielding multiphasic emf-/ht-EODs (present in both functional group I and II).

Species optimized to functional group II are known from tropical drainages (*G. tigre*, *G.* n. sp. ALT, *G. varzea*, *G. curupira* and *G. mamiraua*) and also sub-tropical/temperature drainages in which there is a distinct, colder, austral winter (*G. omarorum*, *G. pantanal* and *G.* n. sp. ITU). They are also known from low-conductivity (e.g. *G. curupira*, *G.* n. sp. ALT) and high-conductivity systems (the remaining species) (Table 1).

Morpho-functional group III

The species we assigned to this group (*G. carapo* SU, *G. carapo* WA and *G. sylvius*, all in the *G. carapo*-D clade) exhibit category 3 ht-EODs. Three additional species from the *G. carapo*-D clade for which detailed electrophysiological analyses have not yet been conducted (*G. arapaima*, *G. carapo* CA and *G. ucamara*) exhibit very similar category 3 ht-EODs and likely share similar morpho-functional bases for the EOD. The early positive component P_{-1} (corresponding to V_{1ct}) in this group is suspected to be of neural origin – emanating from the posterior electromotor nerve, which is especially thick in this group. Species in the *G. carapo*-D clade include the largest of all *Gymnotus* (with most species reaching more than 300 mm total length; Table 1). The need to synchronize the activity of electrocytes separated by more than ca. 300 mm away may require thicker axons, generating larger compound action potentials for increasing conduction speed. The largest of the species we analyzed (*G. arapaima*) has the highest average P_{-1} amplitude (and highest proportion of individuals with P_{-1} present in the ht-EOD).

As with functional group II, species in functional group III are known from both tropical (*G. carapo* SU, *G. carapo* CA, *G. arapaima*, *G. carapo* WA and *G. ucamara*) and subtropical/temperate systems (*G. sylvius*). All of these species appear to have relatively cosmopolitan ecological distributions – occurring in both low- and high-conductivity systems (in contrast with species in all the other functional groups, which seem to occur either in low- or high-conductivity systems, but not both). We are unaware of any aspect of the emf-EOD or EO anatomy of functional group III that should facilitate tolerance of wider conductivity ranges.

Morpho-functional group IV

The unusual anatomy and emf-EOD of *G. obscurus* (with its characteristic quasi-monophasic category 4 ht-EOD) represents a derived condition, nested deeply within a region of the *Gymnotus* phylogeny otherwise optimized to functional group II (Fig. 1B).

The drastic loss of EOD complexity appears to have resulted from a loss of rostral innervation in the dorsal row of the EO, and from modifications of the shapes of the electrocytes to disc-shaped units not seen in any of the other functional groups (all other examined taxa have drum-shaped electrocytes). Double innervation is found in all the remaining 10 species for which we conducted morpho-functional surveys, and given that it is the condition in functional groups I and II, at the basal divergence of the genus, it is likely the plesiomorphic condition in the genus.

All known larval *Gymnotus* generate quasi-monophasic category 4 ht-EODs (Crampton and Hopkins, 2005; Crampton et al., 2011; Pereira et al., 2007). It is therefore tempting to speculate that the origin of quasi-monophasic adult EODs in *G. obscurus* involved paedomorphic retention of an ancestral larval EOD. However, drum-shaped, double innervated electrocytes are clearly present in quasi-monophasic larval *G. omarorum* (Pereira et al., 2007), indicating that double innervation is expressed earlier in ontogeny than the appearance of multiphasic waveforms. If double-innervated electrocytes are present in larvae from all *Gymnotus* species, this would definitely rule out paedomorphic retention of mono-innervated electrocytes as an explanation for quasi-monophasy in *G. obscurus*.

In addition to the case of *G. obscurus*, there are two other independent transitions from a character state optimized to multiphasic category 2 ht-EODs, to quasi-monophasic category 4 ht-EODs: first in *G. henni* from the Pacific coast of Colombia, and second in *G. cylindricus* + *G. maculosus* from Central America. Kirschbaum (Kirschbaum, 1995) (fig. 8.8 therein) noted that the dorsal row of electrocytes in *G. cylindricus* is 'apparently not innervated rostrally', and commented on the irregular arrangement and shape of the electrocytes. Kirschbaum's observations suggest that the evolution of the category 4 ht-EOD in *G. cylindricus* and *G. maculosus* may have involved similar and convergent anatomical modifications to those in *G. obscurus*. However, this needs to be confirmed. Likewise, we know nothing about the anatomical and physiological mechanisms underlying the origin of the category 4 ht-EOD in *G. henni*. All species with category 4 ht-EODs occur in tropical systems with high electrical conductivity.

The category 4 ht-EODs of *Electrophorus* represent an additional, independent evolutionary origin of this EOD condition. As in *G. obscurus*, the electrocytes of *Electrophorus* are monoinnervated and disc-shaped, and show very low auto-excitability on their rostral faces. However, despite these convergent commonalities, given the highly specialized anatomy of the EOs of *Electrophorus*, the mechanisms underlying monophasy are likely distinct from those in *Gymnotus* with category 4 ht-EODs. Due to the uncertainty of the position of the family Gymnotidae (*Electrophorus* + *Gymnotus*) within the Gymnotiformes – see alternative arrangements in Alves-Gomes et al. (Alves-Gomes et al., 1995), Albert (Albert, 2001) and Arnegard et al. (Arnegard et al., 2010b) – we are as yet unable to conclude with confidence whether the condition in *Electrophorus* represents the retention of an ancestral monophasic condition or the transition from a plesiomorphic multiphasic state.

A major conclusion of these analyses is that the phylogenetic distribution of functional groups I through IV exhibits a close correspondence with the ht-EOD categories 1 through 4 (i.e. I with 1, II with 2, III with 3, IV with 4). With the exception of *G. cylindricus*, *G. maculosus* and *G. henni*, there is a precise correspondence between the optimizations in Fig. 1A and 1B. Such is the tightness of this correlation that we can make reasonable predictions about the functional group status of species that are equivocal (or likely to have been incorrectly optimized) in Fig. 1B. Based on ht-EODs, we predict that: (1) *G. jonasi* belongs to functional group I; (2) *G. pantherinus* and members of the *G. cataniapo* group belong to functional group II; (3) members of the *G. carapo*-C clade also belong to functional group II; and (4) *G. henni*, *G. cylindricus* and *G. maculosus* belong to functional group IV (or convergent variants of it). These predictions will be tested by our ongoing morpho-functional surveys of *Gymnotus*.

We also note that during the long evolutionary history of the *Gymnotus* lineage, which diverged from *Electrophorus* ~60 mya (Lovejoy et al., 2010), there have been remarkably few transitions in EOD functional groups. Following a basal divergence between morpho-functional group I and group II (with the ancestral condition unknown), the only transitions that we have reconstructed are from group II to III (twice) and group II to IV (three times). Comparative surveys of the morpho-functional basis of the EOD in a wider diversity of pulse-generating gymnotiform genera will be necessary to determine whether some kinds of transitions in EOD structure are consistently more common than others, and to gain a fuller understanding of the selective pressures and constraints that have shaped signal evolution in the neotropical electric fishes.

Ultimate causes of EOD diversity in *Gymnotus*

Discussions of the ultimate causes of signal evolution in animals usually focus on selective pressures of an extrinsic nature, which are typically divided into abiotic or biotic factors (Bradbury and Vehrencamp, 2011). Abiotic selection on signal design often arises from constraints to signal transmission and reception imposed by the physical structure of the habitat between the sender and receiver (Seehausen et al., 2008; Tobias et al., 2010). Biotic selection on signal design arises from the presence of other animals that generate or receive signals of the same modality, including both conspecifics and closely related heterospecifics, or predators/parasites (which may be very distantly related) that can locate an animal by its signal. Selective forces of an intrinsic nature, for developmentally robust and energetically efficient integration of the signal generation and reception system, are typically not considered because they are impossible to test for (in comparison to assessable external selective forces), and because they are assumed to be inextricably linked to multiple other body systems (Bradbury and Vehrencamp, 2011; Gerhardt, 1999; Niven and Laughlin, 2008).

In this section we review some of the known or postulated extrinsic ultimate causes of diversity of electric signals in *Gymnotus*, with emphasis on the ht-EOD.

Abiotic selection pressures on *Gymnotus* signals

In animals with acoustic or visual communication signals, there is abundant evidence for frequency-dependent variation in transmission performance through different physical habitats – largely as a result of refractive or reflective attenuation. Where species exhibit variation in habitat distributions, this can result in adaptive variation in signal structure [e.g. Tobias et al. (Tobias et al., 2010) for bird calls, and Seehausen et al. (Seehausen et al., 2008) for nuptial colors in fishes]. However, the communication component of electric fish EODs should be relatively unaffected by this kind of 'sensory drive' (*sensu* Boughman, 2002) because, unlike in acoustic and visual signals, electrostatic fields are not distorted between sender and receiver by refraction or reflection, and show no frequency-dependent attenuation with distance (Brenowitz, 1986; Hopkins, 1999b).

Notwithstanding the likely immunity of the communication component of *Gymnotus* EODs to sensory drive, we must also

consider the electrolocation function, which is likely the dominant sensory modality involved in prey detection in *Gymnotus* (Albert and Crampton, 2005). As observed in the echolocation signal of bats (Siemers and Schnitzler, 2004), we might expect variation in the electrolocation component of the EOD to arise from sensory drive for differential electrolocation performance in different microhabitats (or associated with dietary variation). For instance, correlations between the PPF of a species' EOD and its diet or microhabitat have been predicted on theoretical grounds related to the detection of capacitances of electrolocated objects (von der Emde and Ringer, 1992).

Empirical support for correlations between ht-EOD and microhabitat are conspicuously lacking for *Gymnotus*. In the most diverse communities of *Gymnotus* studied to date – near Tefé, Brazil (12 species) (Crampton et al., 2011), and Iquitos, Peru (8–9 species), in the Amazon basin – we failed to find correlations between the PPF or waveform of the ht-EOD and salient habitat parameters such as conductivity, dissolved oxygen, substrate type and density, or flow (W.G.R.C., unpublished). Indeed, a relatively homogenous habitat, the rootmat of floating rafts of macrophytes, hosts breeding communities of species with all the major waveform types known for the genus: ht-EOD category 1: *G. jonasi*; category 2: *G. varzea* and *G. mamiraua*; category 3: *G. arapaima* and *G. carapo* CA; and category 4: *G. obscurus*. Considering all species of *Gymnotus*, across the entire geographical range of the genus, there are also no clear correlations between ht-EOD waveform or PPF and habitat.

We propose that the absence of correlations between ht-EOD structure and habitat is because, as outlined earlier, the ht-EOD is predominantly a proxy for the communication component of the signal generated from the central portion of the EO, and not the rostrally generated electrolocation component. Comparative data are as yet unavailable to test whether aspects of the short-range rostral electrolocation component of the EOD (measurable in the emf-EOD) instead correlate to habitat.

Biotic selection pressures on *Gymnotus* signals

Predator avoidance

The mate attraction signals of animals may attract predators, typically resulting in a trade-off between natural selection for crypsis and sexual selection for conspicuous, ornamental signals (Ryan, 1985; Stoddard, 2002). In the electrosensory modality, EODs may attract passively electroreceptive predators, notably catfishes and *Electrophorus*, which possess ampullary electroreceptors that are maximally sensitive to low-frequency energy (LFE) at around 0–0.03 kHz. The EODs of larval *Gymnotus* are quasi-monophasic (Crampton and Hopkins, 2005; Crampton et al., 2011; Pereira et al., 2007), and are dominated by LFE in the range sensitive to ampullary electroreceptors (see Fig. 9A), but except for species belonging to ht-EOD category 4, these conspicuous EODs are transformed early in development into multiphasic EODs. The appearance of a large negative phase following the P_1 (V_3) phase elevates the PPF, and suppresses the contribution of LFE to the signal. At the same time, the net DC component of the ht-EOD, which is also conspicuous to electroreceptive predators, is suppressed by balancing the positive and negative components of the signal until the net current between the curve of the ht-EOD waveform and 0 V is close to zero. By these two mechanisms the transition from quasi-monophasic to multiphasic signals 'cloaks' LFE (Stoddard, 1999; Stoddard and Markham, 2008) at a stage where the EOD amplitude is rapidly increasing with body size (Pereira et al., 2007). Stoddard (Stoddard, 1999) hypothesized that selection from electroreceptive predators accounts for both the early ontogenetic transition to multiphasic signals observed in most pulse-generating gymnotiforms, and also the evolutionary origins of multiphasic signals from a plesiomorphic monophasic adult condition; note, however, that the phylogenies of Lovejoy et al. (Lovejoy et al., 2010) and Arnegard et al. (Arnegard et al., 2010b) do not support the notion of an ancestral monophasic EOD.

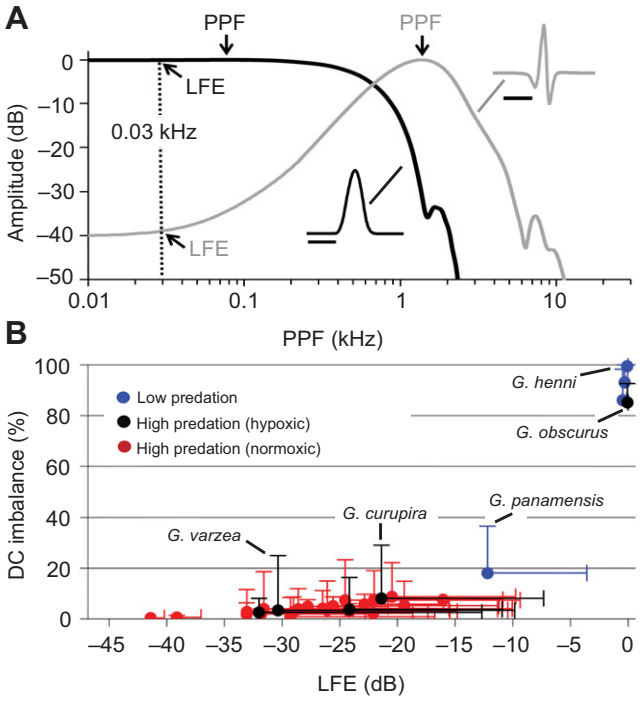

Fig. 9. Conspicuousness of *Gymnotus* EODs to electroreceptive predators (data from K. Brochu, W.G.R.C., J. A. Maldonado-Ocampo and N.R.L., unpublished). (A) Power spectral density plots of a monophasic ht-EOD (black plots and symbols) and multiphasic ht-EOD (gray plots and symbols). LFE, low-frequency energy, a measure of conspicuousness to electroreceptive predators, quantified as signal amplitude (dB) at 0.03 kHz, with peak power frequency (PPF) of signal scaled to 0 dB. (B) LFE plotted against DC imbalance of the signal, another measure of conspicuousness to electroreceptive predators, for 30 *Gymnotus* species. DC imbalance is quantified by measuring the area under each of the phase waveforms in the (P_1-normalized) ht-EOD, and then calculating {[(abs *x*/abs∫all phases)–0.5]×200} (where *x*=∫negative phases or ∫positive phases, whichever has the greater absolute value). Error bars represent the maximum values for each species. For descriptions of the 'low predation' and 'high predation' systems occupied by *Gymnotus*, see 'Biotic selection pressures on *Gymnotus* signals'.

Fig. 9 shows interspecific variation in the theoretical conspicuousness of *Gymnotus* ht-EODs to electroreceptive predators. Conspicuousness can be quantified using two metrics: first, LFE, as the amplitude in the power spectral density of the ht-EOD at 0.03 kHz (in dB), with PPF of the signal scaled to 0 dB; and second, DC imbalance, as a percentage value representing ht-EOD symmetry, from 0% (areas of the positive phases perfectly match the areas of the negative phases) to 100% (ht-EOD purely monophasic). The data in Fig. 9 illustrate that most species of *Gymnotus* have relatively inconspicuous ht-EODs, with low levels of LFE (means mostly below −20 dB from the PPF) and little DC imbalance (means mostly less than 5% imbalanced, with extreme outliers typically less than 10%). In contrast, five species exhibit

highly conspicuous ht-EODs: *G. henni*, *G. maculosus*, *G. cylindricus*, *G. panamensis* and *G. obscurus*. Four of these species have quasi-monophasic category 4 ht-EODs, while *G. panamensis*, which is the sister taxon to the quasi-monophasic species pair *G. cylindricus* + *G. maculosus*, is the only multiphasic species to exhibit significantly higher mean LFE and DC imbalance than congeners. Below we distinguish between 'conspicuous' (*G. panamensis* and all ht-EOD category 4 species) and 'cryptic' taxa (all other *Gymnotus*).

In light of *Gymnotus* phylogeny, conspicuous ht-EODs have evolved three times independently from cryptic ancestors (Fig. 1A). Based on the geographic and ecological distribution of the conspicuous lineages, Brochu (Brochu, 2011) proposed that these transitions are a consequence of predator release combined with sexual selection and sensory bias. Large pimelodid catfishes and electric eels are absent from the Pacific coastal drainages of South America, and all drainages of Central America, including the río Atrato (a Caribbean drainage in which *G. choco* and *G. henni* occur). In these systems the only potential electroreceptive predator of *Gymnotus* is the heptapterid *Rhamdia*, which is a small-bodied omnivorous catfish that likely would only predate small juveniles; note that *Gymnotus* is known to form nests which it guards zealously from such predators (Crampton and Hopkins, 2005). Six *Gymnotus* species occur in these predator-free systems (labeled 'low predation' in Fig. 9): *G. cylindricus*, *G. maculosus* and *G. panamensis* in Central America, and *G. choco*, *G. henni* and *G. esmeraldas* in Pacific coastal Panama, Colombia and Ecuador. The ht-EODs of *G. choco* and *G. esmeraldas* are unknown, but remarkably, all the other species have conspicuous EODs (see above), representing two independent transitions from an ancestral cryptic state. In contrast, the Atlantic coast drainages of South America, including the Magdalena and Maracaibo (which are trans-Andean systems), and all major cis-Andean systems (excepting some small coastal drainages of Brazil) are known to have electroreceptive predators – either large piscivorous catfishes such as *Pseudoplatystoma* and/or *Electrophorus*. In these 'high predation' systems, of the 26 species for which we have obtained ht-EODs (Table 1), all have cryptic signals except for one: *G. obscurus* (discussed below). This evidence supports the hypothesis that selective pressure from electroreceptive predators favors cryptic signals, while predator-free environments allow the evolution of more conspicuous signals in *Gymnotus*.

While predator release explains the potential for evolution of conspicuous signals, we still need to explain why in predator-free zones, DC-balanced multiphasic signals were not simply retained. Brochu (Brochu, 2011) proposed that a pre-existing sensory bias (Fuller et al., 2005) in females for low-frequency signals is a plausible mechanism for the origins of quasi-monophasic signals in both males and females of *Gymnotus* species with conspicuous signals. Among the cryptic species found in high predation areas, some species exhibit a subtle, but significant, sexual dimorphism of the ht-EOD – for example, *G. coatesi* and *G. curupira* (Crampton et al., 2011) (and see 'Sexual selection', below) – in which the LFE content of male signals is high relative to females. Female sensory bias for low frequencies also appears to be prevalent throughout the other myogenic gymnotiform families (Sternopygidae, Hypopomidae, Rhamphichthyidae), where instances of ht-EOD sexual dimorphism always involve lower frequencies in males (Crampton and Albert, 2006). Under conditions of predator release, constraints on the expression of LFE in male signals would be relaxed. Female choice for low-frequency EODs, in the absence of antagonistic selection from predators, could ultimately lead to the evolution of quasi-monophasic signals, which have the highest possible expression of LFE.

The conspicuous signal in *G. obscurus*, a cis-Andean species, is perplexing. This species is restricted to hypoxic floodplain systems, in which large pimelodid catfishes (but not electric eels) are absent or rare. But there are many species of *Gymnotus* with cryptic signals that also occupy hypoxic habitats (see Table 1). We note that two species of *Gymnotus* which occur in hypoxic systems (*G. curupira* in terra firme swamps, and *G. varzea* in whitewater floodplains), exhibit considerable LFE and DC imbalance in reproductive males (see outliers labeled in Fig. 9B), which supports the notion that conspicuous signal elements may be more likely to evolve in hypoxic systems with putatively lower predation rates. An alternative explanation for the existence of quasi-monophasic ht-EODs in weakly electric cis-Andean species was proposed by Stoddard (Stoddard, 1999). He speculated that the quasi-monophasic ht-EODs of a floodplain-dwelling species of *Brachyhypopomus* ('sp. 2') may be indicative of Batesian mimicry (in which a benign species is avoided by predators or competitors because it resembles a dangerous species) of *Electrophorus*, which has similar ht-EODs. Nonetheless, we consider this hypothesis unlikely (including for *G. obscurus*, which occurs in syntopy with *Brachyhypopomus* 'sp. 2'), because *Brachyhypopomus* 'sp. 2' (the putative mimic) is by far the most common species of gymnotiform in the lakes and flooded forests of whitewater floodplain systems, greatly exceeding *Electrophorus* (the putative model) in abundance. Where a model is rare relative to a mimic, selection to avoid the model and any mimics should be weak, therefore disfavoring the evolution and maintenance of mimicry (Huheey, 1964; Pfennig et al., 2001).

Selection from reproductive interference

Errors in recognition between species (or divergent populations) that have confusingly similar signals can lead to heterospecific 'mismating' events (Gröning and Hochkirch, 2008). Another kind of reproductive interference is masking interference (jamming), where spectral overlap between the signals of two species results in an impairment of the ability to locate or communicate with conspecifics (Amézquita et al., 2006). Both kinds of reproductive interference can promote reproductive character displacement (RCD) – the evolutionary divergence of signals (and associated receiver apparatus) between taxa in areas of geographical sympatry (Gerhardt, 1999).

We do not expect jamming to be a significant impetus for evolutionary change in *Gymnotus* because the phenomenon occurs only over short distances (Pereira et al., 2012), and yet individual *Gymnotus* are invariably well spaced in the wild: all species are apparently highly territorial. In contrast, there are strong grounds to suggest that selection against mismating may be an important cause of signal divergences in *Gymnotus*. Crampton et al. (Crampton et al., 2011) reported an unusual case of RCD in *Gymnotus* from the Tefé region of the Central Amazon. This involves a pattern in which the ht-EODs of *Gymnotus* exhibit more partitioning in a multivariate signal space representing ht-EOD waveform structure after maturation than before, and moreover, species pairs that were close neighbors in signal space before maturation exhibited significantly greater divergence during maturation than species pairs that were well spaced before maturation. Crampton et al. (Crampton et al., 2011) argued that these patterns arose in response to selection against maladaptive heterospecific mismating events, thereby reducing errors in species recognition. A forthcoming paper will demonstrate a similar case of RCD involving a different set of species in the Peruvian

Amazon, suggesting that the case in the Tefé region is not an isolated phenomenon.

Species of *Gymnotus* in regional sympatric communities invariably exhibit a non-overlapping distribution in signal space. In low-diversity communities, species are often partitioned by the PPF alone (see Rodríguez-Cattáneo et al., 2008), which may offer a ready means for species recognition *via* electroreceptor tuning properties. However, in more complex regional assemblages, such as the species-rich *Gymnotus* community of the Tefé region, PPFs overlap among reproductive males in a manner suggesting that species recognition must involve the discrimination not only of peak spectral properties of the communication component of the EOD, but also aspects of waveform shape (Crampton et al., 2011). The ability for gymnotiforms to discriminate spectral from temporal properties of EODs has been demonstrated empirically in hypopomids (Heiligenberg and Altes, 1978).

We have also observed geographical variation in the signal structure of widely distributed species. It is likely that selection against mismating acts on single species in a contextual manner, depending upon the particular combination of species they co-occur with in each regional assemblage. Combined with non-adaptive drift, this is expected to lead to a mosaic of population-level variation in signal structure across a wide geographical arena. This kind of variation may lead to reproductive isolation on secondary contact, acting as an engine for speciation in the genus. Future efforts will expand this theme in a phylogenetic context.

Much work is also required to understand the mechanisms by which *Gymnotus* recognize and discriminate mates in the context of mate choice. For instance, is the ht-EOD waveform alone sufficient to encode species and sex, or do modulations in the pulse rate during courtship provide additional cues for recognition? *Gymnotus* are known to produce complex modulations of the EOD pulse rate during territorial interactions (Black-Cleworth, 1970; Westby, 1974), but nothing is known about sexual EOD modulations in *Gymnotus*, and the extent to which they may be species specific. Likewise, do aspects of the electric field close to a signaling fish contain species- or sex-specific information that is not detectable to a potential mate further away – especially near the periphery of electrocommunication range where a pair first encounter each other's signals?

Sexual selection

Sexual selection – either by mate choice or inter-sexual conflict – commonly promotes the evolution of costly ornamental signal components that evolve in spite of, or even because of, these costs (including conspicuousness to predators), because they serve as honest indices of male quality (Maynard Smith and Harper, 2003). Under some circumstances, sexual selection is thought to promote divergences of mate attraction signals among closely related species, including in electric fishes (Arnegard et al., 2010a; Boul et al., 2007). Little is known of the mechanisms underlying sexual selection in *Gymnotus*, but a small number of species exhibit sexually dimorphic ht-EODs in which LFE is significantly boosted in males (i.e. as conspicuous ornaments) by an elongation of the P_2 (V_4) and reduction of P_3 (V_5) [see Crampton et al. (Crampton et al., 2011), fig. 4 therein, for examples from *G. curupira* and *G. coatesi*]. These EOD modifications are observed only in sexually mature males, and likely result from hormonal influences on EOD auto-excitability, particularly on EOD components V_4 and V_5 (see 'Interspecific diversity in the EO and emf-EOD', and Fig. 5). In comparison to other myogenic gymnotiforms, sexual EOD dimorphism is apparently relatively uncommon in *Gymnotus* (known only in *G. coatesi*, *G. curupira*, *G. javari*, *G. panamensis* and *G. varzea*, although data from multiple mature males and females are unavailable for many species) and also relatively subtle, involving small changes in waveform shape.

Conclusions

Differences in ht-EODs between closely related *Gymnotus* species generally consist of variations in EOD duration (which approximate to variation in PPF) and variation in the relative size and amplitude of EOD components. However, we also observed several more substantial evolutionary transitions in ht-EOD structure, including three independent transitions to quasi-monophasic ht-EODs. At the proximate level, variation in ht-EODs corresponds mostly to diversity in innervation patterns of the electrocytes, auto-excitability, electrocyte density and distribution, and the expression of neurogenic components in the EOD. These characters can be categorized into four distinct morpho-functional groups, which exhibit a strong phylogenetic signal and a close correlation to the structure of the ht-EOD. At the ultimate level, extrinsic selective pressures of a biotic nature – electroreceptive predators, reproductive interference with heterospecifics and sexual selection – all appear to play roles in shaping the communication component of the EOD of *Gymnotus*. However, unlike in many acoustic and visual animal signaling systems, selection from the abiotic environment does not appear to be an important source of diversifying selection of the communication signal.

Acknowledgements

For discussions and assistance we thank P. Aguilera, J. Albert, E. Birmingham, D. Bloom, K. Brochu, M. Castelló, E. Cilleruelo, E. Correa, M. Guevara, L. Iribarne, J. Lambert, F. Lima, J. Maldonado-Ocampo, J. Mol, C. Nagamachi, J. Oliveira, A. Orfinger, H. Ortega, A. Pastorino, C. Pereira, M. Richer-de-Forges and J. Waddell.

Author contributions

A.A.C., W.G.R.C. and N.R.L contributed to conception and design of the long term study. A.A.C. and A.R.-C. conducted the morpho-functional studies. W.G.R.C. conducted the comparative survey of head-to-tail EODs. W.G.R.C. and N.R.L. conducted the taxonomic and phylogenetic studies. W.G.R.C., A.A.C. and N.R.L. drafted the article and contributed to its revision.

Competing interests

No competing interests declared.

Funding

This research was funded by the National Science Foundation [grant DEB-0614334 'Evolution of species and signal diversity in the Neotropical electric fish *Gymnotus*' to PI W.G.R.C., and Co-PIs A.A.C., N.R.L. and J. Albert; grant DEB-1146374 to W.G.R.C.]; the Canadian National Science and Engineering Research Council [Discovery grant to N.R.L.]; the European Commission [grant N231845 ICT-FET, 'ANGELS' to A.A.C.]; and PEDECIBA [grants to A.A.C. and doctoral fellowship to A.R.-C.].

References

Aguilera, P. A. and Caputi, A. A. (2003). Electroreception in *G. carapo*: detection of changes in waveform of the electrosensory signals. *J. Exp. Biol.* **206**, 989-998.

Aguilera, P. A., Castelló, M. E. and Caputi, A. A. (2001). Electroreception in *Gymnotus carapo*: differences between self-generated and conspecific-generated signal carriers. *J. Exp. Biol.* **204**, 185-198.

Albe-Fessard, D. and Chagas, C. (1954). Etude de la sommation à la jonction nerf-électroplaque chez le Gymnote (*Electrophorus electricus*). *J. Physiol.* **46**, 823-840.

Albe-Fessard, D. and Chagas, C. (1955). Études par dérivation intracellulaire des effets sommatifs de deux stimulations nerveuses successives au niveau d'une électroplaque du Gymnote. *C R Acad. Sci. III* **239**, 1951-1954.

Albe-Fessard, D. and Martins-Ferreira, H. (1953). Role de la commande nerveuse dans la synchronisation du fonctionnement des élements de l'organe électrique du gymnote, *Electrophorus electricus* L. *J. Physiol.* **45**, 533-546.

Albert, J. S. (2001). Species diversity and phylogenetic systematics of American knifefishes (Gymnotiformes, Teleostei). *Misc. Publ. Mus. Zool. Univ. Michigan* **190**, 1-127.

Albert, J. S. and Crampton, W. G. R. (2001). Five new species of *Gymnotus* (Teleostei: Gymnotiformes) from an Upper Amazonian floodplain, with descriptions of electric organ discharges and ecology. *Ichthyol. Explor. Freshwat.* **12**, 241-266.
Albert, J. S. and Crampton, W. G. R. (2003). Seven new species of the neotropical electric fish *Gymnotus* (Teleostei, Gymnotiformes) with a redescription of *G. carapo* (Linnaeus). *Zootaxa* **287**, 1-54.
Albert, J. S. and Crampton, W. G. R. (2005). Electroreception and electrogenesis. In *The Physiology of Fishes*, 3rd edn (ed. D. Evans), pp. 431-472. New York, NY: CRC Press.
Albert, J. S., Crampton, W. G. R., Thorsen, D. H. and Lovejoy, N. R. (2005). Phylogenetic systematics and historical biogeography of the neotropical electric fish *Gymnotus* (Gymnotidae: Teleostei). *Syst. Biodivers.* **2**, 375-417.
Altamirano, M., Coates, C. W., Grundfest, H. and Nachmansohn, D. (1953). Mechanisms of bioelectric activity in electric tissue. I. The response to indirect and direct stimulation of electroplaques of *Electrophorus electricus*. *J. Gen. Physiol.* **37**, 91-110.
Alves-Gomes, J. A., Ortí, G., Haygood, M., Heiligenberg, W. and Meyer, A. (1995). Phylogenetic analysis of the South American electric fishes (order Gymnotiformes) and the evolution of their electrogenic system: a synthesis based on morphology, electrophysiology, and mitochondrial sequence data. *Mol. Biol. Evol.* **12**, 298-318.
Amézquita, A., Hödl, W., Lima, A. P., Castellanos, L., Erdtmann, L. and de Araújo, M. C. (2006). Masking interference and the evolution of the acoustic communication system in the Amazonian dendrobatid frog *Allobates femoralis*. *Evolution* **60**, 1874-1887.
Arnegard, M. E., McIntyre, P. B., Harmon, L. J., Zelditch, M. L., Crampton, W. G. R., Davis, J. K., Sullivan, J. P., Lavoué, S. and Hopkins, C. D. (2010a). Sexual signal evolution outpaces ecological divergence during electric fish species radiation. *Am. Nat.* **176**, 335-356.
Arnegard, M. E., Zwickl, D. J., Lu, Y. and Zakon, H. H. (2010b). Old gene duplication facilitates origin and diversification of an innovative communication system – twice. *Proc. Natl. Acad. Sci. USA* **107**, 22172-22177.
Bell, C. C., Bradbury, J. and Russell, C. J. (1976). The electric organ of a mormyrid as a current and voltage source. *J. Comp. Physiol. A* **110**, 65-88.
Bennett, M. V. L. (1971). Electric organs. In *Fish Physiology* (ed. W. S. Hoar and D. J. Randall), pp. 347-484. New York, NY: Academic Press.
Bennett, M. V. L. and Grundfest, H. (1959). Electrophysiology of electric organ in *Gymnotus carapo*. *J. Gen. Physiol.* **42**, 1067-1104.
Black-Cleworth, P. (1970). The role of electric discharges in the non-reproductive social behaviour of *Gymnotus carapo*. *Anim. Behav. Monogr.* **3**, 1-77.
Boughman, J. W. (2002). How sensory drive can promote speciation. *Trends Ecol. Evol.* **17**, 571-577.
Boul, K. E., Funk, W. C., Darst, C. R., Cannatella, D. C. and Ryan, M. J. (2007). Sexual selection drives speciation in an Amazonian frog. *Proc. R. Soc. B* **274**, 399-406.
Bradbury, J. W. and Vehrencamp, S. L. (2011). *Principles of Animal Communication*, 2nd edn. Sunderland, MA: Sinauer Associates, Inc.
Brenowitz, E. A. (1986). Environmental influences on acoustic and electric animal communication. *Brain Behav. Evol.* **28**, 32-42.
Brochu, K. (2011). *Molecular Phylogenetics of the Neotropical Electric Knifefish Genus Gymnotus (Gymnotidae, Teleostei): Biogeography and Signal Evolution of the Trans-Andean Species*. MSc thesis, University of Toronto, Toronto, ON.
Bullock, T. H., Hopkins, C. D., Popper, A. N. and Fay, R. R. (2005). *Electroreception*. New York, NY: Springer.
Caputi, A. A. and Aguilera, P. (1996). A field potential analysis of the electromotor system in *Gymnotus carapo*. *J. Comp. Physiol. A* **179**, 827-835.
Caputi, A. A. and Nogueira, J. (2012). Identifying self- and nonself-generated signals: lessons from electrosensory systems. In *Sensing in Nature* (ed. C. López-Larrea), pp. 107-125. New York, NY: Springer.
Caputi, A. A. and Trujillo-Cenóz, O. (1994). The spinal cord of *Gymnotus carapo*: the electromotoneurons and their projection patterns. *Brain Behav. Evol.* **44**, 166-174.
Caputi, A. A., Macadar, O. and Trujillo-Cenóz, O. (1989). Waveform generation of the electric organ discharge in Gymnotus carapo. 3. analysis of the fish body as an electric source. *J. Comp. Physiol. A* **165**, 361-370.
Caputi, A. A., Macadar, O. and Trujillo-Cenóz, O. (1994). Waveform generation in *Rhamphichthys rostratus* (L.) (Teleostei, Gymnotiformes). *J. Comp. Physiol. A* **174**, 633-642.
Caputi, A. A., Silva, A. C. and Macadar, O. (1998). The electric organ discharge of *Brachyhypopomus pinnicaudatus*. The effects of environmental variables on waveform generation. *Brain Behav. Evol.* **52**, 148-158.
Caputi, A. A., Aguilera, P. A. and Castelló, M. E. (2003). Probability and amplitude of novelty responses as a function of the change in contrast of the reafferent image in *G. carapo*. *J. Exp. Biol.* **206**, 999-1010.
Castelló, M. E., Aguilera, P. A., Trujillo-Cenóz, O. and Caputi, A. A. (2000). Electroreception in *Gymnotus carapo*: pre-receptor processing and the distribution of electroreceptor types. *J. Exp. Biol.* **203**, 3279-3287.
Castelló, M. E., Rodríguez-Cattáneo, A., Aguilera, P. A., Iribarne, L., Pereira, A. C. and Caputi, A. A. (2009). Waveform generation in the weakly electric fish *Gymnotus coropinae* (Hoedeman): the electric organ and the electric organ discharge. *J. Exp. Biol.* **212**, 1351-1364.
Crampton, W. G. R. (1998). Electric signal design and habitat preferences in a species rich assemblage of gymnotiform fishes from the Upper Amazon basin. *An. Acad. Bras. Cienc.* **70**, 805-847.
Crampton, W. G. R. (2006). Evolution of electric signal diversity in gymnotiform fishes. II. Signal design. In *Communication in Fishes* (ed. F. Ladich, S. P. Collin, P. Moller and B. G. Kapoor), pp. 697-731. Enfield, NH: Science Publishers.
Crampton, W. G. R. (2011). An ecological perspective on diversity and distributions In *Historical Biogeography of Neotropical Freshwater Fishes* (ed. J. S. Albert and R. E. Reis), pp. 165-189. Berkeley, CA: University of California Press.
Crampton, W. G. R. and Albert, J. S. (2006). Evolution of electric signal diversity in gymnotiform fishes. I. Phylogenetic systematics, ecology and biogeography. In *Communication in Fishes* (ed. F. Ladich, S. P. Collin, P. Moller and B. G. Kapoor), pp. 647-696; 718-731. Enfield, NH: Science Publishers.
Crampton, W. G. R. and Hopkins, C. D. (2005). Nesting and paternal care in the weakly electric fish *Gymnotus* (Gymnotiformes: Gymnotidae) with descriptions of larval and adult electric organ discharges of two species. *Copeia* **2005**, 48-60.
Crampton, W. G. R., Thorsen, D. H. and Albert, J. S. (2005). Three new species from a diverse, sympatric assemblage of the electric fish *Gymnotus* (Gymnotiformes, Gymnotidae) in the lowland Amazon basin, with notes on ecology. *Copeia* **2005**, 82-99.
Crampton, W. G. R., Davis, J. K., Lovejoy, N. R. and Pensky, M. (2008). Multivariate classification of animal communication signals: a simulation-based comparison of alternative signal processing procedures using electric fishes. *J. Physiol. Paris* **102**, 304-321.
Crampton, W. G. R., Lovejoy, N. R. and Waddell, J. C. (2011). Reproductive character displacement and signal ontogeny in a sympatric assemblage of electric fish. *Evolution* **65**, 1650-1666.
Donaldson, P. E. K. (1958). *Electronic Apparatus for Biological Research*. London: Butterworth.
Fuller, R. C., Houle, D. and Travis, J. (2005). Sensory bias as an explanation for the evolution of mate preferences. *Am. Nat.* **166**, 437-446.
Gerhardt, H. C. (1999). Reproductive character displacement and other sources of selection on acoustic communication systems. In *The Design of Animal Communication* (ed. M. D. Hauser and M. Konishi), pp. 515-534. Cambridge, MA: MIT Press.
Gröning, J. and Hochkirch, A. (2008). Reproductive interference between animal species. *Q. Rev. Biol.* **83**, 257-282.
Grundfest, H. (1961). Ionic mechanisms in electrogenesis. *Ann. New York Acad. Sci.* **94**, 405-457.
Hagedorn, M. and Carr, C. (1985). Single electroctyes produce a sexually dimorphic signal in South American electric fish, *Hypopomus occidentalis* (Gymnotiformes, Hypopomidae). *J. Comp. Physiol. A* **156**, 511-523.
Heiligenberg, W. and Altes, R. A. (1978). Phase sensitivity in electroreception. *Science* **199**, 1001-1004.
Hopkins, C. D. (1999a). Design features for electric communication. *J. Exp. Biol.* **202**, 1217-1228.
Hopkins, C. D. (1999b). Signal evolution in electric communication. In *The Design of Animal Communication* (ed. M. D. Hauser and M. Konishi), pp. 461-491. Cambridge, MA: MIT Press.
Hopkins, C. D. (2005). Passive electrolocation. In *Electroreception* (ed. T. H. Bullock, C. D. Hopkins, A. N. Popper and R. R. Fay), pp. 264-289. New York, NY: Springer.
Huheey, J. E. (1964). Studies of warning coloration and mimicry. IV. A mathematical model of model-mimic frequencies. *Ecology* **45**, 185-188.
Kirschbaum, F. (1995). Discharge types of gymnotiform fishes. In *Electric Fishes: History and Behavior* (ed. P. Moller), pp. 172-180. London: Chapman and Hall.
Knudsen, E. I. (1975). Spatial aspects of the electric fields generated by weakly electric fish. *J. Comp. Physiol. A* **99**, 103-118.
Lorenzo, D., Velluti, J. C. and Macadar, O. (1988). Electrophysiological properties of abdominal electrocytes in the weakly electric fish *Gymnotus carapo*. *J. Comp. Physiol. A* **162**, 141-144.
Lorenzo, D., Sierra, F., Silva, A. and Macadar, O. (1990). Spinal mechanisms of electric organ discharge synchronization in *Gymnotus carapo*. *J. Comp. Physiol. A* **167**, 447-452.
Lorenzo, D., Sierra, F., Silva, A. and Macadar, O. (1993). Spatial distribution of the medullary command signal within the electric organ of *Gymnotus carapo*. *J. Comp. Physiol. A* **173**, 221-226.
Lovejoy, N. R., Lester, K., Crampton, W. G. R., Marques, F. P. L. and Albert, J. S. (2010). Phylogeny, biogeography, and electric signal evolution of neotropical knifefishes of the genus *Gymnotus* (Osteichthyes: Gymnotidae). *Mol. Phylogenet. Evol.* **54**, 278-290.
Macadar, O., Lorenzo, D. and Velluti, J. C. (1989). Waveform generation of the electric organ discharge in *Gymnotus carapo* II. Electrophysiological properties of single electrocytes. *J. Comp. Physiol. A* **165**, 353-360.
Mago-Leccia, F. (1994). *Electric Fishes of the Continental Waters of America*. Caracas: Biblioteca de la Academia de Ciencias Fisicas, Matematicas y Naturales.
Markham, M. R. and Stoddard, P. K. (2005). Adrenocorticotropic hormone enhances the masculinity of an electric communication signal by modulating the waveform and timing of action potentials within individual cells. *J. Neurosci.* **25**, 8746-8754.
Markham, M. R., McAnelly, M. L., Stoddard, P. K. and Zakon, H. H. (2009). Circadian and social cues regulate ion channel trafficking. *PLoS Biol.* **7**, e1000203.
Maynard Smith, J. and Harper, D. (2003). *Animal Signals*. Oxford: Oxford University Press.
Mayr, E. (1961). Cause and effect in biology. *Science* **134**, 1501-1506.
McGregor, P. K. and Westby, G. W. M. (1993). Individually characteristic EOD waveforms and discrimination by *Gymnotus carapo*. *J. Comp. Physiol. A* **173**, 741.
Milhomem, S. S. R., Pieczarka, J. C., Crampton, W. G. R., Silva, D. S., de Souza, A. C. P. and Carvalho, J. R. (2008). Chromosomal evidence for a putative cryptic species in the *Gymnotus carapo* species-complex (Gymnotiformes, Gymnotidae). *BMC Genetics* **9**, 75.
Niven, J. E. and Laughlin, S. B. (2008). Energy limitation as a selective pressure on the evolution of sensory systems. *J. Exp. Biol.* **211**, 1792-1804.
Pereira, A. C., Rodríguez-Cattáneo, A., Castelló, M. E. and Caputi, A. A. (2007). Post-natal development of the electromotor system in a pulse gymnotid electric fish. *J. Exp. Biol.* **210**, 800-814.
Pereira, A. C., Aguilera, P. and Caputi, A. A. (2012). The active electrosensory range of *Gymnotus omarorum*. *J. Exp. Biol.* **215**, 3266-3280.
Pfennig, D. W., Harcombe, W. R. and Pfennig, K. S. (2001). Frequency-dependent Batesian mimicry. *Nature* **410**, 323.
Richer-de-Forges, M. M., Crampton, W. G. R. and Albert, J. S. (2009). A new species of *Gymnotus* (Gymnotiformes, Gymnotidae) from Uruguay: description of a model species in neurophysiological research. *Copeia* **2009**, 538-544.

Rodríguez-Cattáneo, A. and Caputi, A. A. (2009). Waveform diversity of electric organ discharges: the role of electric organ auto-excitability in *Gymnotus* spp. *J. Exp. Biol.* **212**, 3478-3489.
Rodríguez-Cattáneo, A., Pereira, A. C., Aguilera, P. A., Crampton, W. G. R. and Caputi, A. A. (2008). Species-specificity of a fixed motor pattern: the electric organ discharge of *Gymnotus*. *PLoS ONE* **3**, e2038.
Rodríguez-Cattáneo, A., Aguilera, P., Cilleruelo, E., Crampton, W. G. and Caputi, A. A. (2013). Electric organ discharge diversity in the genus *Gymnotus*: anatomo-functional groups and electrogenic mechanisms. *J. Exp. Biol.* **216**, 1501-1515.
Ryan, M. J. (1985). *The Tungara Frog: A Study in Sexual Selection and Communication.* Chicago, IL: University of Chicago Press.
Seehausen, O., Terai, Y., Magalhaes, I. S., Carleton, K. L., Mrosso, H. D. J., Miyagi, R., van der Sluijs, I., Schneider, M. V., Maan, M. E., Tachida, H. et al. (2008). Speciation through sensory drive in cichlid fish. *Nature* **455**, 620-626.
Siemers, B. M. and Schnitzler, H. U. (2004). Echolocation signals reflect niche differentiation in five sympatric congeneric bat species. *Nature* **429**, 657-661.
Sierra, F., Comas, V., Buño, W. and Macadar, O. (2005). Sodium-dependent plateau potentials in electrocytes of the electric fish Gymnotus carapo. *J. Comp. Physiol. A* **191**, 1-11.
Sierra, F., Comas, V., Buño, W. and Macadar, O. (2007). Voltage-gated potassium conductances in *Gymnotus* electrocytes. *Neuroscience* **145**, 453-463.
Stoddard, P. K. (1999). Predation enhances complexity in the evolution of electric fish signals. *Nature* **400**, 254-256.
Stoddard, P. K. (2002). The evolutionary origins of electric signal complexity. *J. Physiol. Paris* **96**, 485-491.
Stoddard, P. K. and Markham, M. R. (2008). Signal cloaking by electric fish. *Bioscience* **58**, 415-425.
Sullivan, J. P., Lavoué, S. and Hopkins, C. D. (2002). Discovery and phylogenetic analysis of a riverine species flock of African electric fishes (Mormyridae: Teleostei). *Evolution* **56**, 597-616.
Szabo, T. (1961). Les organes électrique de *Gymnotus carapo*. *Koninkl. Ned. Akad. Wetenschap.* **64**, 584-586.
Tobias, J. A., Aben, J., Brumfield, R. T., Derryberry, E. P., Halfwerk, W., Slabbekoorn, H. and Seddon, N. (2010). Song divergence by sensory drive in Amazonian birds. *Evolution* **64**, 2820-2839.
Trujillo-Cenóz, O. and Echagüe, J. A. (1989). Waveform generation of the electric organ discharge in *Gymnotus carapo*. I. Morphology and innervation of the electric organ. *J. Comp. Physiol. A* **165**, 343-351.
Trujillo-Cenóz, O., Echagüe, J. A. and Macadar, O. (1984). Innervation pattern and electric organ discharge waveform in *Gymnotus carapo* (Teleostei; Gymnotiformes). *J. Neurobiol.* **15**, 273-281.
von der Emde, G. and Ringer, T. (1992). Electrolocation of capacitive objects in four species of pulse-type weakly electric fish. I. Discrimination performance. *Ethology* **91**, 326-338.
Westby, G. W. M. (1975). Further analysis of the individual discharge characteristics predicting social dominance in the electric fish *Gymnotus carapo*. *Anim. Behav.* **23**, 249-260.